Large circular hydrophone arrays for long-range monitoring of North Atlantic right whales: first deployments and testing in the Gulf of St. Lawrence

Yvan Simard, Kevin Duquette, Philippe Royer, Nathalie Roy, Michel Rousseau, Clément Juif, Cédric Gervaise, and Charlotte Constans

Fisheries and Oceans Canada
Maurice Lamontagne Institute
850 route de la Mer, P.O. Box 1000
Mont-Joli, Québec
Canada G5H 3Z4

2022

Canadian Technical Report of
Fisheries and Aquatic Sciences 3491

Fisheries and Oceans Canada | Pêches et Océans Canada

Canada

Canadian Technical Report of Fisheries and Aquatic Sciences

Technical reports contain scientific and technical information that contributes to existing knowledge but which is not normally appropriate for primary literature Technical reports are directed primarily toward a worldwide audience and have an international distribution. No restriction is placed on subject matter and the series reflects the broad interests and policies of Fisheries and Oceans Canada, namely, fisheries and aquatic sciences.

Technical reports may be cited as full publications. The correct citation appears above the abstract of each report. Each report is abstracted in the data base *Aquatic Sciences and Fisheries Abstracts*.

Technical reports are produced regionally but are numbered nationally. Requests for individual reports will be filled by the issuing establishment listed on the front cover and title page.

Numbers 1-456 in this series were issued as Technical Reports of the Fisheries Research Board of Canada. Numbers 457-714 were issued as Department of the Environment, Fisheries and Marine Service, Research and Development Directorate Technical Reports. Numbers 715-924 were issued as Department of Fisheries and Environment, Fisheries and Marine Service Technical Reports. The current series name was changed with report number 925.

Rapport technique canadien des sciences halieutiques et aquatiques

Les rapports techniques contiennent des renseignements scientifiques et techniques qui constituent une contribution aux connaissances actuelles, mais qui ne sont pas normalement appropriés pour la publication dans un journal scientifique. Les rapports techniques sont destinés essentiellement à un public international et ils sont distribués à cet échelon. II n'y a aucune restriction quant au sujet; de fait, la série reflète la vaste gamme des intérêts et des politiques de Pêches et Océans Canada, c'est-à-dire les sciences halieutiques et aquatiques.

Les rapports techniques peuvent être cités comme des publications à part entière Le titre exact figure au-dessus du résumé de chaque rapport. Les rapports techniques sont résumés dans la base de données *Résumés des sciences aquatiques et halieutiques*.

Les rapports techniques sont produits à l'échelon régional, mais numérotés à l'échelon national. Les demandes de rapports seront satisfaites par l'établissement auteur dont le nom figure sur la couverture et la page du titre.

Les numéros 1 à 456 de cette série ont été publiés à titre de Rapports techniques de l'Office des recherches sur les pêcheries du Canada. Les numéros 457 à 714 sont parus à titre de Rapports techniques de la Direction générale de la recherche et du développement, Service des pêches et de la mer, ministère de l'Environnement. Les numéros 715 à 924 ont été publiés à titre de Rapports techniques du Service des pêches et de la mer, ministère des Pêches et de l'Environnement. Le nom actuel de la série a été établi lors de la parution du numéro 925.

Canadian Technical Report of
Fisheries and Aquatic Sciences 3491

2022

LARGE CIRCULAR HYDROPHONE ARRAYS FOR LONG-RANGE MONITORING OF NORTH ATLANTIC RIGHT WHALES: FIRST DEPLOYMENTS AND TESTING IN THE GULF OF ST. LAWRENCE

by

Yvan Simard[1], Kevin Duquette[1], Philippe Royer[1], Nathalie Roy[1], Michel Rousseau[1], Clément Juif[1], Cédric Gervaise[2], and Charlotte Constans[2]

[1]Fisheries and Oceans Canada
Maurice Lamontagne Institute
850 route de la Mer, P.O. Box 1000
Mont-Joli, Québec
Canada G5H 3Z4

[2] SENSEAFR
5 Rue Gallice
38100 Grenoble
France

© Her Majesty the Queen in Right of Canada, 2022
Cat. No. Fs97-6/3491E-PDF ISBN 978-0-660-44035-4 ISSN 1488-5379

Correct citation for this publication:

Simard, Y., Duquette, K., Royer, P., Roy, N., Rousseau, M., Juif, C., Gervaise, C., and Constans, C. 2022. Large circular hydrophone arrays for long-range monitoring of North Atlantic right whales: first deployments and testing in the Gulf of St. Lawrence. Can. Tech. Rep. Fish. Aquat. Sci. 3491: viii + 40 p.

TABLE OF CONTENTS

Page

LIST OF TABLES

LIST OF FIGURES

ABSTRACT

Simard, Y., Duquette, K., Royer, P., Roy, N., Rousseau, M., Juif, C., Gervaise, C., and Constans, C. 2022. Large circular hydrophone arrays for long-range monitoring of North Atlantic right whales: first deployments and testing in the Gulf of St. Lawrence. Can. Tech. Rep. Fish. Aquat. Sci. 3491: viii + 40 p.

To respond to the needs of continuously monitoring North Atlantic Right Whales (NARW) in real time over large areas of the Gulf of St. Lawrence, performance studies using simulations of *in situ* conditions (Gervaise et al. 2019a, 2019b; Gervaise et al. 2021) have concluded that the optimal passive acoustic monitoring (PAM) systems were large circular hydrophone arrays. To accomplish this PAM challenge and position the whales in their habitat, two prototypes of such circular hydrophone arrays, 20 m in diameter, were designed, built, and tested off the Gaspé peninsula in the summer of 2021. This report presents the characteristics of this new PAM technology, used for the first time to track low frequency calling whales over large-scale sensitive areas of their habitats. These large apparatus were positioned on the seafloor, at significant distances from the coast, and depths exceeding human diver ranges. The deployment techniques, involving coordinated boats, are detailed. The approach used is discussed and recommendations for further improvements are provided. Examples of preliminary results confirming the performance studies are presented for several species of baleen whales and a transiting merchant ship. Further steps for real-time implementation will be detailed in further contributions from this research project.

RÉSUMÉ

Simard, Y., Duquette, K., Royer, P., Roy, N., Rousseau, M., Juif, C., Gervaise, C., and Constans, C. 2022. Large circular hydrophone arrays for long-range monitoring of North Atlantic right whales: first deployments and testing in the Gulf of St. Lawrence. Can. Tech. Rep. Fish. Aquat. Sci. 3491: viii + 40 p.

Pour répondre au besoin de monitorer les baleines noires de l'Atlantique Nord (NARW) en temps réel sur de grandes étendues du Golfe du Saint-Laurent, des études de performance utilisant des simulations des conditions *in situ* (Gervaise et al. 2019a, 2019b; Gervaise et al. 2021) ont conclu que l'usage de grands réseaux circulaires d'hydrophones était le système optimal de monitorage par acoustique passive (PAM). Pour relever ce défi PAM et positionner les baleines dans leur habitat, deux prototypes de tels réseaux circulaires d'hydrophones, de 20 m de diamètre, ont été conçus, construits et testés au large de la péninsule gaspésienne à l'été 2021. Ce rapport présente les caractéristiques de cette nouvelle technologie PAM, utilisée pour la première fois pour suivre les baleines communiquant avec des sons de basses fréquences sur de grandes distances dans des aires sensibles de leur habitat. Ces appareils de grande taille ont été mis en place sur les fonds marins, à des distances considérables de la côte et des profondeurs inaccessibles en plongée par l'homme. Les techniques utilisées pour les déployer à l'aide de bateaux coordonnés sont fournies. L'approche utilisée est discutée et des recommandations d'améliorations sont fournies. Des exemples de résultats préliminaires confirmant les études de performance sont présentés pour plusieurs espèces de baleines à fanons ainsi que pour un navire marchand en transit. Des travaux connexes en vue d'une mise en œuvre en temps réel seront détaillés dans des contributions ultérieures de ce projet de recherche.

ACRONYMS

AAV:	Anse-à-Valleau array site
AIS:	Automatic Identification System
AR:	Array Receiver
CLD:	Cloridorme array site
CTD:	Conductivity, Temperature, Depth
DASA:	DFO Acoustic Surveillance Array
DFO:	Department of Fisheries and Oceans
GSL:	Gulf of St. Lawrence
HDPE:	High-Density Polyethylene
HF:	High-Frequency
LF:	Low-Frequency
MLI:	Maurice Lamontagne Institute
MLB:	Mal-Bay array site
NARW:	North Atlantic Right Whale
PAM:	Passive Acoustics Monitoring
PRC:	Percé array site
PSD:	Power Spectral Density
RHIB:	Rigid-Hull Inflatable Boat
RL:	Received Level
SARA:	Species At Risk Act
SL:	Source Level
SNR:	Signal-to-Noise Ratio
TB:	Terabyte
TC:	Transport Canada
TDOA:	Time Difference of Arrival
TL:	Transmission Loss
WBR:	Whale Binaural Rings

1. INTRODUCTION

1.1 NARW current context and threats in Gulf of St. Lawrence

The North Atlantic right whale (*Eubalaena glacialis*) (NARW) is a small population (~ 350 ind., (Pettis et al. 2021)) that has an Endangered status under the Canadian Species at Risk Act (SARA) (DFO 2014). It used to be present during summer in the Atlantic off Nova Scotia and Newfoundland, especially at the mouth of the Bay of Fundy. Occasional presence of a few individuals in the Gulf of St. Lawrence (GSL) drastically shifted in 2015 to become an annual occurrence of a large proportion of the population during the ice-free period (DFO 2018, Simard et al. 2019). Following significant mortality events in 2017 and 2019 (Bourque et al. 2020; Daoust et al. 2017), the Canadian government has put in place protective measures to minimize mortality risk, by imposing time-space restrictions of fixed gear fishing and of vessel speeds in areas of high NARW occurrence (DFO 2019, Transport Canada 2019). These management measures include static zones, where the measures are enforced for the season of NARW presence, and dynamic management areas, where the restriction measures are triggered by the presence of a whale.

The NARW distribution information is then obtained from visual observations using dedicated airplane surveys or from opportunistic sightings reported by boats. These observing means are providing information for a part of the GSL, for whales that are visible at the surface during daytime under favorable weather conditions. The time-space observation effort for a given area is however very low because of the low repetition rate and the small duration of the observation from the moving platforms. To increase the monitoring effort in selected areas and complement the limited visual observation effort and get quasi-continuous information of NARW presence, real-time passive acoustic monitoring (PAM) systems detecting specific NARW upsweep contact calls have been deployed from fixed buoys in ocean observing systems (DFO Viking-WOW buoys, https://ogsl.ca/viking/) and mobile platforms (Slocum glider, https://whalemap.ocean.dal.ca/WhaleMap/).

1.2 PAM with circular hydrophone arrays

Since the PAM systems for monitoring whale presence from their specific calls depend on the signal-to-noise ratio (SNR), their spatial and temporal performance in anthropized oceanic areas on continental shelves is affected by the dominant manmade noise, which is notably originating from chronic shipping traffic (e.g.,Hatch et al. 2008). This is especially true for the contact call characterizing NARW, whose central acoustic frequency (~ 150 Hz, (Parks and Tyack 2005)) is overlapping with the peak frequency band of shipping noise (Clark et al. 2009; Simard et al. 2016). As the GSL is crossed by a continental shipping route, the St. Lawrence Seaway, monitoring NARW in this ecosystem from PAM techniques represents a higher challenge than for other areas of NARW life domain with lower exposure to shipping traffic.

To identify the optimal system to accomplish this task in large areas of the GSL intensively used by NARW, the performance of different PAM systems were compared using realistic numerical simulations taking into account the observed in situ conditions, as well as the characteristics of different acoustic systems, deployment platforms, and signal processing methods

(Gervaise et al. 2019a, 2019b; Gervaise et al. 2021). These studies concluded that large (radius > 10 m) circular hydrophone arrays offered the highest performance for NARW detection and localization over large areas. These synchronized acoustic systems considerably enhance the signal-to-noise ratio by both magnifying the signal and reducing the noise level, especially when the noise sources are well localized, such as for ships, where their azimuths differ from the source azimuth. This capacity is offered by beamforming processing techniques, which coherently sum the signals recorded by each hydrophone, in the time and frequency band of interest, while accounting for the time difference of arrivals (*tdoa*) between the hydrophones as function of the potential azimuths. This summation is performed for several sets of *tdoa*s, each corresponding to a given direction around the array (i.e., the beams). The source azimuth is the direction producing the highest total energy in the frequency band of the targeted source and the signal coming from this direction may be estimated with beamforming techniques. The signal strength enhancement of hydrophone arrays, compared to single-hydrophone recordings, comes from the multiplication of the number of hydrophones. The reduction of the background noise levels is due to the destructive summation of the acoustic signals from interfering sources (e.g., ships) in directions other than the azimuth of the targeted source. This processing results in cancelling the directional noise from occasional ships while beaming towards the direction of the calling NARW. This method is sketched out below (Figure 1).

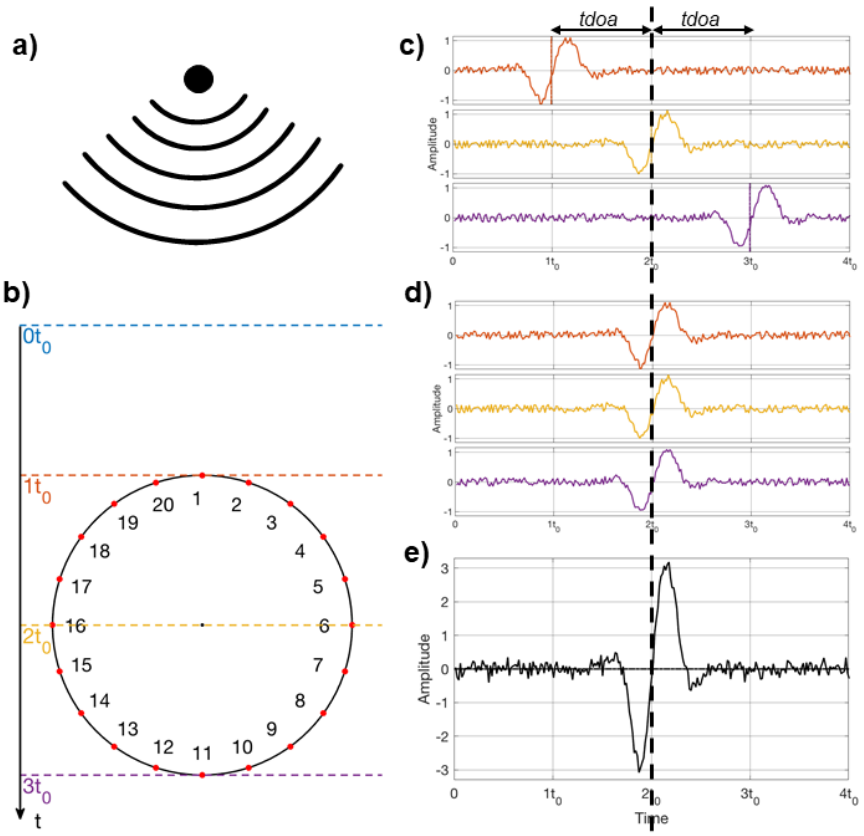

Figure 1. Scheme of the simple beamforming technique from a circular hydrophone array that is traversed by a plane wave (b) radiating from a distant source (a).
c) the wave propagating over the array is crossing the hydrophones at different times (ex.: $1t_0$, $2t_0$, $3t_0$); these delays (*tdoa*) are accounted for (d) in summing the measures (i.e., for a subset of 3 hydrophones in this example) to get the resulting enhanced signal in (e).

Using a pair of such arrays looking from different positions along the coast, the location of the whale can be obtained by crossing the two bearings pointing towards the source. We called such PAM systems: *whale binaural rings* (Whale-B-Rings, or WBR).

Sites for favorable implementation of such WBR PAM systems along the coast of the Gaspé Peninsula to detect and localize NARW were explored in the Honguedo strait, between the peninsula and Anticosti Island, and in their foraging area in northern Shediac through, east of the peninsula (Figure 2). The locations of the sites along the coast were selected for their possibility of cabling the arrays to the shore with a short cable (< ~2 km) for their eventual operation in real-time.

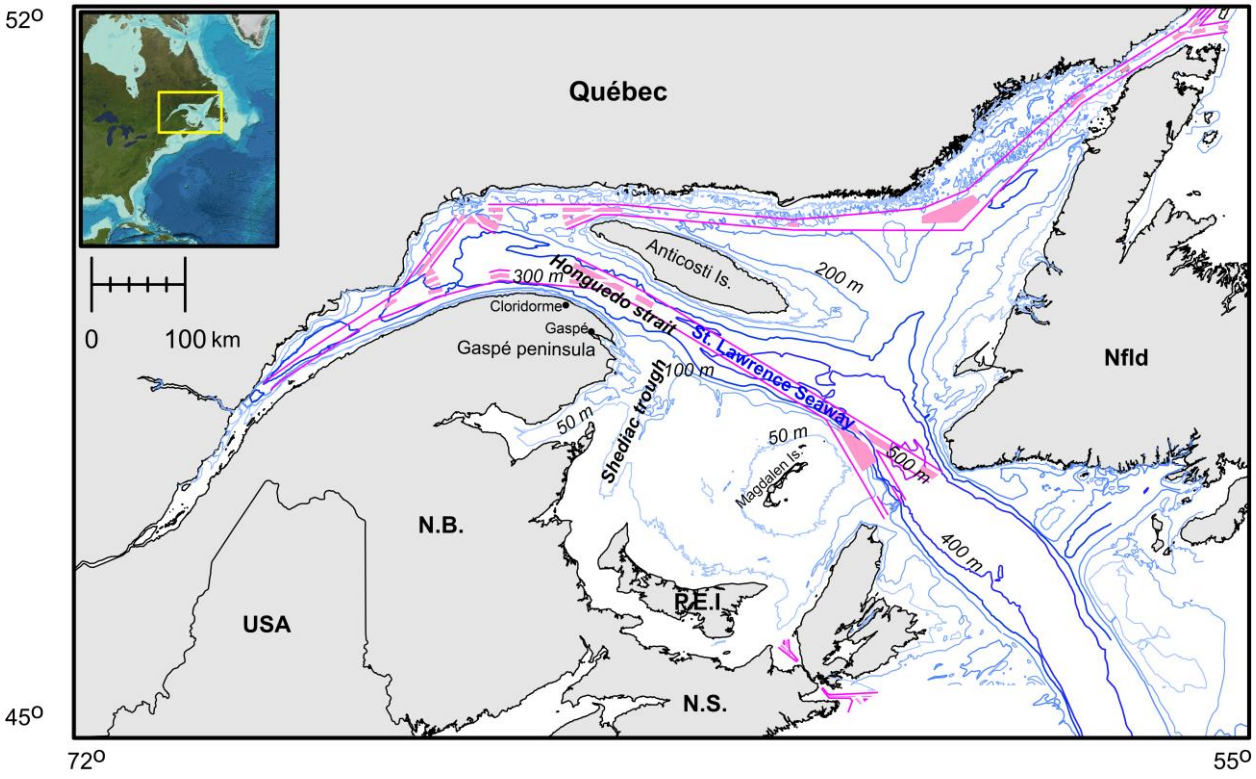

Figure 2. Map of the Gulf of St. Lawrence with the location of the Honguedo strait and Shediac through areas, the bathymetry (blue lines), and the seaways (pink).

Following these preliminary steps, the WBR implementation phase was initiated in 2020 to develop this technology and start sea trials.

The first phase of this project, covering 2020-21, was therefore devoted to the following activities:

- Planning and purchasing the instrumentation,
- Designing, building, and mounting the circular frames to support the hydrophone arrays,
- Testing the hydrophone arrays in a pool,
- Determining the methodology for deploying and recovering the moorings,

- Choosing positions of 4 mooring sites for the array pairs for monitoring NARW in the Honguedo strait and Northern Shediac through areas,
- Deployment of the WBR pairs and recording sounds over a few weeks, for each of these 2 areas,
- Performing an initial data exploration, analysis, and study examples of recorded sounds (from NARW, but also from other whales and other sources of sounds such as ships).

1.3 Organisation of the report

This report first provides a technical description of each part of the WBR array assemblies, followed by a detailed description of the unconventional mooring steps. It then presents an overview of the field measurements, collected data and preliminary results of detection and localization of different mysticete species. A brief discussion of the overall experiment follows and suggestions for improvements and future developments are provided. An appendix supplies details on field measurements such as conductivity, temperature and depth (CTD) profiles, sound speed cross sections, and sounds emitted by a low-frequency projector abord the research vessels for future references.

2. ARRAYS DESCRIPTION AND CIRCULAR ASSEMBLY

2.1 Hydrophone arrays and recording system

The 2 identical hydrophone arrays, named 'DFO Acoustic Surveillance Array' or DASA, were manufactured by Omnitech (https://omnitechelectronics.ca/products/arrays/dasa-2591/). Each array consists of 20 low-frequency (LF) digital hydrophones, distributed at 3.14 m intervals along a 62.8-m portion of a 75-m long cable. This allows configuring the hydrophones around a 20-m diameter circular frame, leaving a 12.2-m cable length for the connection to a control unit (Figure 3). In addition, the system has 4 high-frequency (HF) hydrophones, linked to the control unit by individual cables allowing their placement at even distances along the circular frame of the array, one per quadrant. Their signals are digitized by 4 analog-to-digital converters in the array control unit, the Array Receiver (AR). The 5 cables are connected to this AR, which is powered by a series of 36 VDC battery packs.

LF hydrophones are manufactured by Omnitech (OEI) and calibrated by the Neptune Sonar calibration facility in the UK. Their sensitivity is -193.5 ± 3 dB re 1 V / µPa over the 0-5 kHz frequency range. They are set to sample with a resolution of 24 bits at a rate of 10,000 samples s^{-1}. The amplification gain can be varied by 10-dB steps, from 0 dB to 60 dB. A fixed gain of 40 dB was chosen for our 2021 experiment. Each of the LF hydrophones is protected by a high-density polyethylene (HDPE) plastic shroud, perforated with many holes (Figure 4, left).

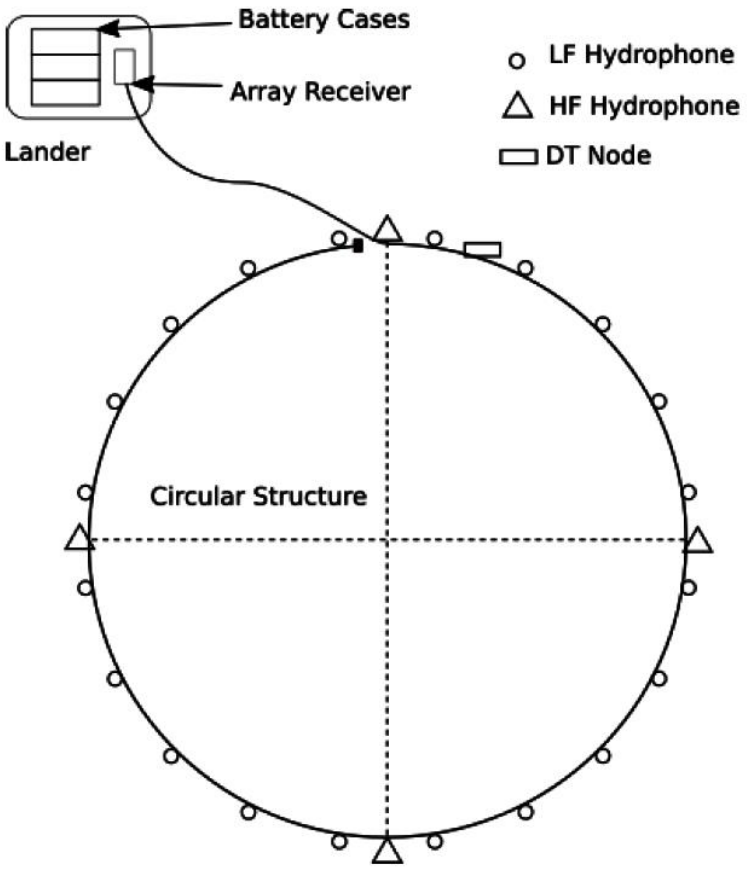

Figure 3. Diagram of a circular hydrophone array connected to a receiver and powered by batteries. The array diameter is 20 m.

The 4 HF hydrophones are TC4032s manufactured and calibrated by Reson (http://www.teledynemarine.com/hydrophones/hydrophones-reson). Their sensitivity is -172 ± 6 dB re 1 V/µPa between 5 Hz and 100 kHz. A 40-dB gain was used during our 2021 experiment. Their signal was digitized with a 24-bit resolution at a rate of 256,000 samples s^{-1}. They are supplied with 4 cable assemblies of different lengths to accommodate their positions on the circular array. To optimize sound reception, these 4 hydrophones are attached vertically on the array with a HDPE support and protection guard (Figure 4, right).

A depth and temperature (DT) node is installed along the LF hydrophone array cable.

The AR controls the array, records the data, and handles all data transfers and communications from the array system to shore (with an optional cable). It includes a connection with an (optional) acoustic modem for underwater wireless remote operation monitoring. The AR data storage can hold up to 4 serial ATA hard drives. We used 4 Samsung Evo Pro 2 TB (Terabyte) SSDs (solid state drive) for our 2021 experiment, providing an 8-TB storage capacity. The system operating mode includes options for setting the power-on, duty cycles, with separate time sequences for the LF and the HF hydrophones.

2.2 **Circular array frame and structural support**

The hydrophone array is mounted around a 20-sided polygonal frame made of an assembly of 20 fiberglass I-beams, each about 3 m in length. These beams are joined by HDPE junctions on which rests a plate (Figure 4 left, Figure 5b) for fixing the hydrophone. Ten steel tension cables, 0.25-inch diameter, consolidate the structure by linking the circular frame to a central HDPE ring (Figure 4 center, Figure 5a). The array cables and hydrophones are attached to the fiberglass and HDPE frame using tie-wraps (Figure 4 left).

Figure 4. Details of the hydrophone array mounting on the circular frame.
Left: LF hydrophone in its shroud, attached on the HDPE plate.
Center: central HDPE ring with attached tension cables and VEMCO VR2AR acoustic release.
Right: view of a vertically mounted HF hydrophone with protective guard, and the inflated tube under the fiberglass structure.

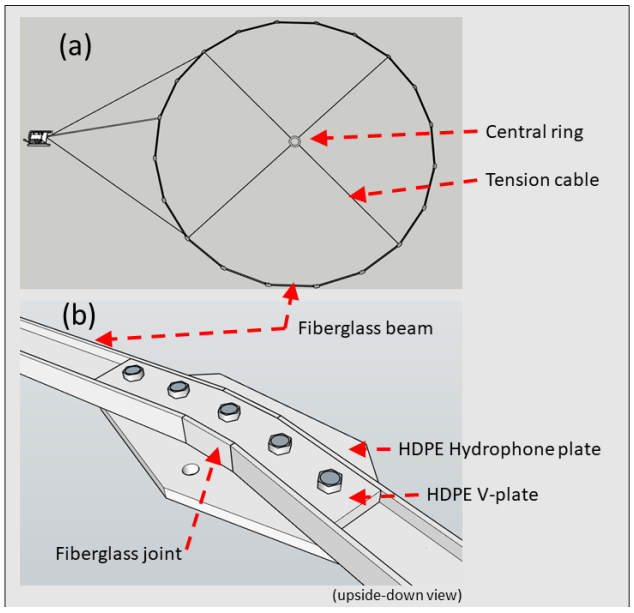

Figure 5. Circular array frame scheme.
a) view of the 20-sided polygon frame of the circular array with the central ring and attached tension cables. b) detailed view of the I-beam joints.

2.3 **Recovery lines**

Sixty-meter long recovery lines (8,800 kg strength ropes) join a fanning bridle attached to 5 points on each side of the circular array (Figure 6). These lines serve multiple purposes:

- The towing line is used for towing the array to and from the mooring site; it also holds the 2 air hoses for the in/out air exchanges with the inflatable tube from each side of the circular array.
- The mooring line is used to moor the lander side of the array; it is attached to the lander by a shackle, which also holds the bridle coming from the array.
- Both the towing and the mooring lines end with VEMCO VR2AR acoustic releases (https://www.oceans-research.com/products/receivers/acoustic-monitoring-receivers/vr2ar/), and associated floats and anchor, to recover the array. The mooring line has 2 releases for increased redundancy. A fourth release is attached to the central ring (Figure 4, center) to provide depth information while mooring or retrieving the array and to help position the center of the mooring.
- These lines can also be recovered with a grapple hook if something goes wrong with the release operations.

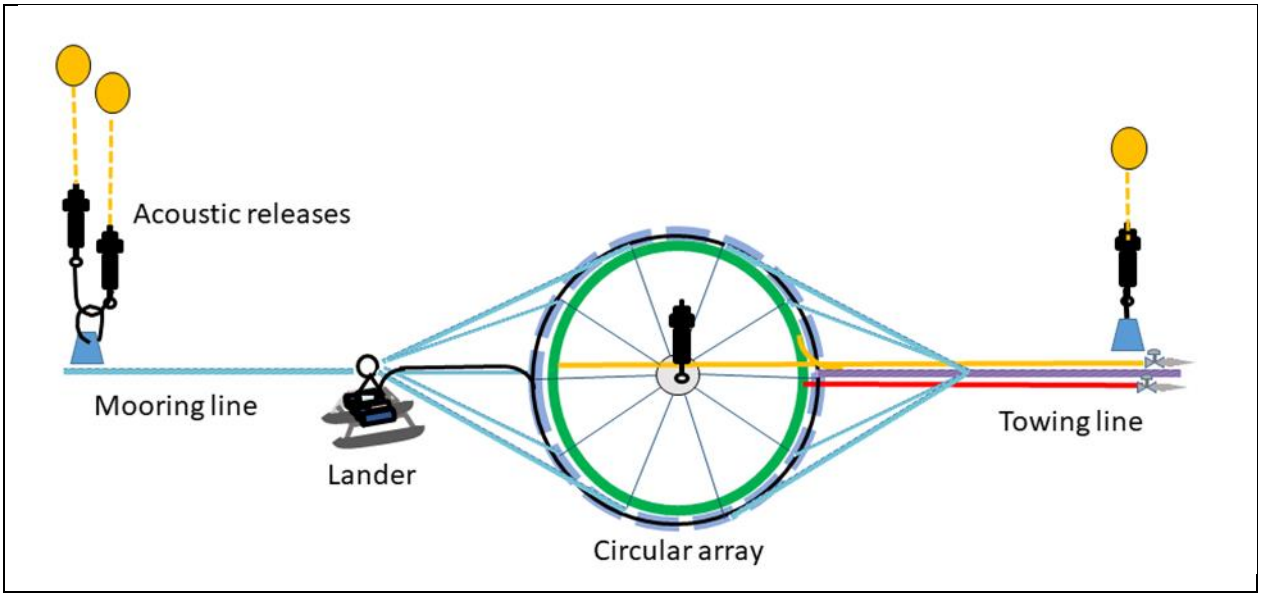

Figure 6. Schematic view of the circular array mooring setup, showing the towing line (in purple), the air lines (in red and yellow) and the mooring line (in blue).
The inflatable resin tube is shown in green. Air is provided by hoses (in yellow and red) connected at both ends of the array. Acoustic releases are installed at the end of each line and one is attached in the middle. Five ropes (in blue), fanning out from each side of the array, provide a bridle attachment to the 20-sided polygonal support of the array.

2.4 **Flotation tube**

To keep the circular array afloat during its transport between the beach and the mooring position by a towing vessel, an inflatable tube was attached under the circular frame. This 75-mm diameter, 61-m long resin tube allows buoyancy adjustments during transport and assists the sinking and recovery maneuverings of the large mooring ensemble. Air hoses were plugged on both sides of this resin tube during the whole mooring operations to control buoyancy by giving/taking air from the tubes. This could be done when the circular array is at the surface or underwater during the recovery. These hoses were attached to the towing line (Figure 6).

2.5 **Lander**

The AR and battery packs are mounted on a sled-lander, made of 0.50-inch stainless steel rod and skis, which can accommodate other instruments such as an acoustic modem (Figure 7). Four (4) battery cases containing each 96 D-cell batteries, providing energy for about 5 weeks at 100% duty cycle, were used during each deployment in 2021.

The weight of this setup is approximately 150 kg in air and 60 kg in water, which requires appropriate ship equipment (winch, pot hauler, deck space) for mooring procedures.

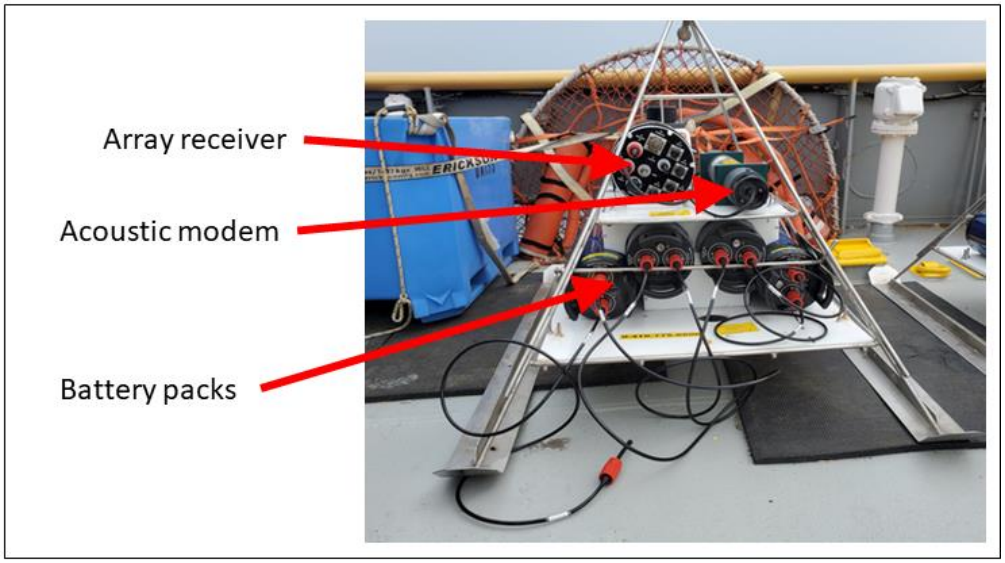

Figure 7. Lander, equipped with the AR, the 4 battery packs and the Teledyne-Benthos acoustic modem.

2.6 **Acoustic modem**

The acoustic modem enables 2-way communication with the AR from the surface. It transmits information to its surface unit about the recording activities and can also perform simple operations remotely. The modem used was an ATM-914 from Teledyne Benthos. It was used to check if the array was still in record mode after deployment.

3. MOORING DEPLOYMENT AND RECOVERY

Because of the large size of the array and the relative flexibility of the circular frame, the following steps were established for transport to the mooring station:

a) Set up the array on a suitable beach (relatively flat and sandy, near the mooring station, accessible by truck; and close to a wharf for docking the towing vessel), ideally at low tide; attach the 5 connection cables to a float in a bundle, while waterproofing the connectors with plastic and electric tape (no waterproof dummy plugs were available).
b) Inflate the resin tube installed under the structure.
c) Drag the array into the water; this requires at least 6 people, 2 equipped with neoprene chest waders to progress in the water (Figure 8a).
d) If the weather is calm and there is enough daylight time left, ideally at high tide slack waters, proceed with the towing. If not, sink the mooring in a few meters of water and anchor it to keep it in standby; when conditions are favorable, the mooring can be quickly put back afloat by inflating the tube.
e) Have a small boat, such as an 8-m Rosborough rigid hull, approach the beach and grab the towing line.
f) Begin slowly towing the structure, at around 1 knot, to the mooring station (Figure 8b), in calm weather conditions.

In the meantime, the mooring vessel is positioned at the station (Figure 8b). It has already on board the lander containing the AR, batteries, and acoustic modem.

Figure 8. Transport of circular hydrophone array to the mooring site.
(a) Dragging the circular hydrophone array into the water from the beach by the team.
(b) Towing of the circular hydrophone array by the small Rosborough vessel. The R/V Coriolis II is visible at a distance, positioned at the mooring station.

When the towing vessel arrives at the mooring station, the deployment steps are the following (cf. Figure 9):

- The 5 cable endings are transferred to the mooring vessel. The array cable is plugged into the AR on the lander, which is then ~10 m from the circular frame of the array. The recording is initiated.
- The mooring line is used to lower the lander. It goes through a pulley on the ship's aft A-frame and is retained by a capstan.
- The towing vessel maneuvers to position the array and extend the cabling about 50 m up current of the desired location for deployment. In the meantime, the lander is immersed and maintained close to the surface, away from the circular frame (Figure 10).
- The towing vessel starts deflating the resin tube to initiate immersion of the array, opening the valves on the towing line hoses (Figure 6).
- Both the mooring and the towing vessels lower the array and attached lander while holding their lines until the bottom is reached. The vessels keep a safe distance apart to insure that the lander keeps its external position relative to the circular fame.
- The vessels move back slowly to spread the lines. Acoustic releases, with attached floats and anchor, are fixed to the line ends and dropped to the bottom.

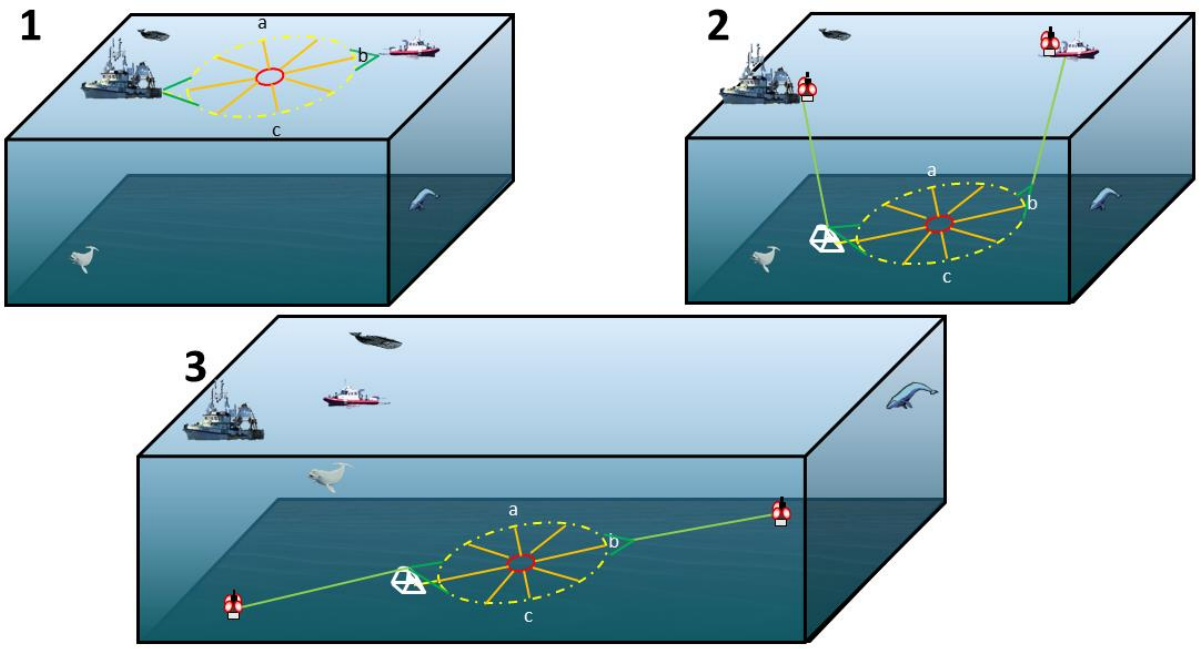

Figure 9. Mooring steps of the circular hydrophone array.
(1) positioning of the mooring at the station, using two vessels;
(2) lowering the array to the bottom; and
(3) deploying the recovery lines with their acoustic release systems.

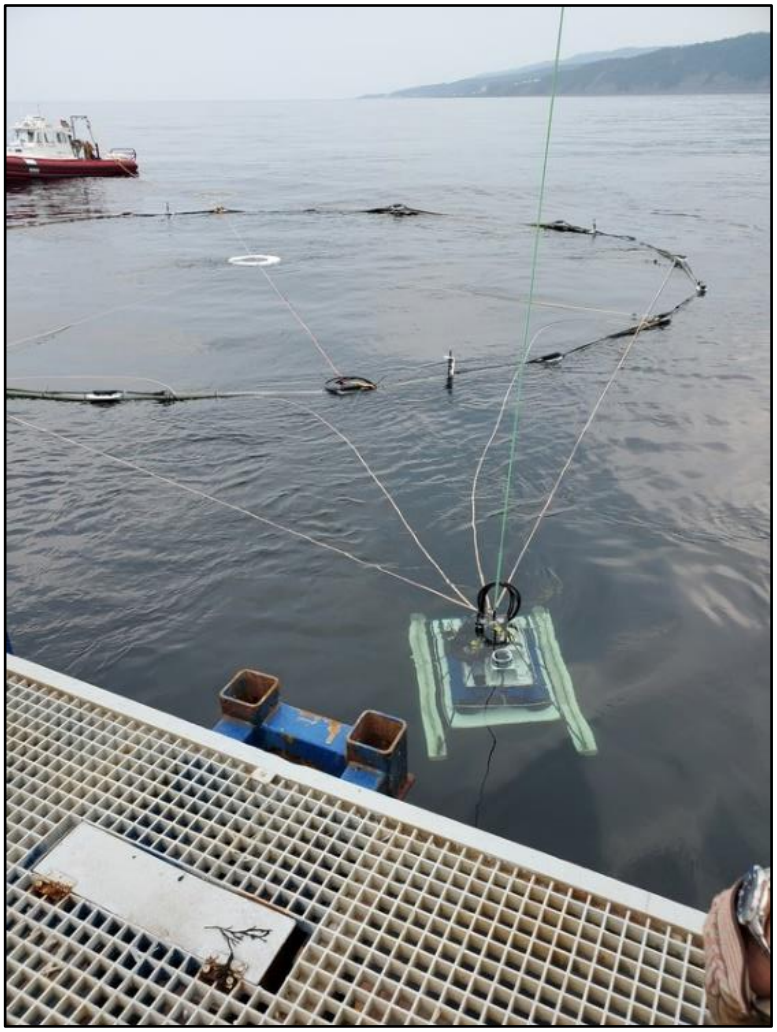

Figure 10. Mooring operations, with circular array and lander at the surface.

Recovering the array follows the above mooring procedures but in reverse order:

- The acoustic releases on both ground lines are triggered. The buoys at line ends then pop up at the surface.
- The two vessels take hold of the lines and synchronously slowly lift the lander and the array up to a depth of about 10 m. A mark on the ground lines indicates that depth. The towing vessel then inflates the inflatable tube under the circular array frame using the 2 air lines.
- The lander and the increasingly buoyant circular array are slowly brought to the surface and guided using both recovery lines.
- The lander is brought aboard the mooring vessel and the recording is stopped on the AR.
- The 5 cable endings are unplugged and attached to a float.
- The towing vessel slowly tows the floating array to bring it back to shore.
- The mooring can be quickly sunk near the beach if time is short to bring it on land, or if the tide is low.

From our experiment, deployment and recovery require calm weather conditions, wind speed less than 10 kn, waves heights not exceeding 1 m, and currents lower than 1 kn.

4. FIELD TEST CHARACTERISTICS AND MEASUREMENTS

4.1 Beaches

Table 1 provides the positions of beaches used for assembling the arrays before deployment on Gaspé peninsula in July and August 2021. Three of these beaches were chosen just next to a small port for convenience. At Percé, the small-vessels wharf was less than 1 nautical mile from the beach.

Table 1. Positions of beaches used for assembling the arrays before deployment.

Station name	Beach name	Longitude		Latitude	
		Deg.	Min.	Deg.	Min.
Anse-à-Valleau	Anse-à-Valleau port	64	32.650	49	4.803
Cloridorme	Cloridorme port	64	51.059	49	11.138
Percé	Anse du Nord	64	12.811	48	31.744
Mal-Bay	Mal-Bay port	64	11.909	48	37.346

4.2 Vessels

The deployment and recovery of the arrays require two vessels that have the capacity for lowering and lifting the arrays (e.g., boom, crane, pot hauler, winch). One of them must have the capacity to launch and bring aboard the 150-kg lander. The other one must have the capacity to inflate/deflate the inflatable tube that enables the array floatation. We have used small (< 15-m) fishing vessels, a 50-m oceanographic ship (R/V Coriolis II) and a Canadian Coast Guard (CCG) 8-m Rosborough 2 x 225 HP outboard RHIB (rigid-hull inflatable boat) (Table 2). This latter boat was used as the towing vessel.

Table 2. Vessels used during field work.

Field work dates	CCG boat	Chartered vessel Type (Name) Length
July 9-15	8-m Rosborough (‘Colvert’, ‘Butor’)	R/V (‘Coriolis II’) 50 m
July 23-30	8-m Rosborough (‘Colvert’)	R/V (‘Coriolis II’) 50 m and Fishing vessel (‘Virginie-Audrey’) 15 m
August 23-26	8-m Rosborough (‘Kildir’)	Fishing vessel (‘Renaissance 93’)

4.3 **Array positions and settings**

Figure 11 shows the 4 positions of the array moorings during the 2021 experiments. Table 3 summarizes their characteristics including deployment periods, depths, and the recording settings. Cloridorme and Anse-à-Valleau formed a first binaural pair of circular arrays that were deployed simultaneously to monitor the Honguedo strait whereas Mal-Bay and Percé formed a second one looking east of the Gaspé peninsula.

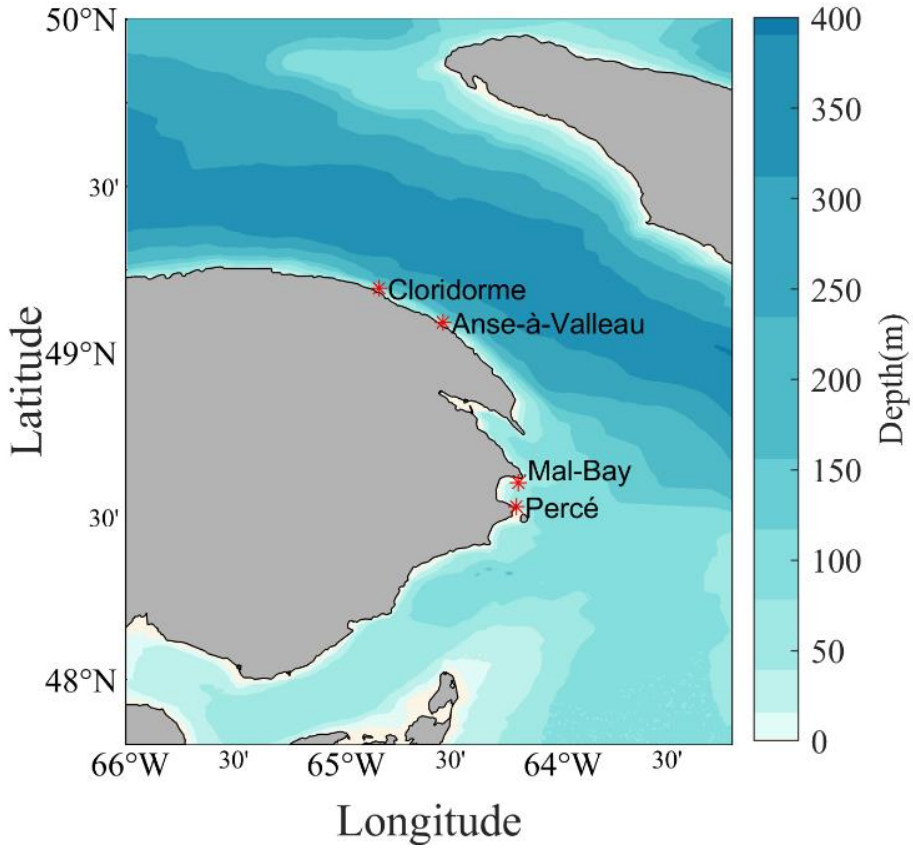

Figure 11. Positions of circular array deployments in July and August 2021.

4.4 **Measurements and data collected**

4.4.1 VEMCO acoustic releases

The 4 VEMCO acoustic releases used on each array mooring have the capacity to detect the VEMCO 69 kHz codes from tagged fishes passing nearby. These fish tracking data were saved for ongoing projects in GSL.

One VEMCO VR2AR was placed in the center of the array (Figure 4 center) for obtaining its overall position using ranging interrogations made with the VEMCO VR100 surface unit deployed from the Rosborough boat at various locations around the array. These measurements complemented the recorded position of the lander (from vessel position) when it was deposited on the seafloor during the deployment.

Table 3. Array deployment and settings used in 2021.
The positions provided here correspond to the ship GPS at the time when the lander was dropped on the bottom.

Array location	**Longitude**		**Latitude**		**Deployment dates**	**Depth (m)**	**LF**		**HF**		**Gain (dB)**
	Deg.	**min**	**Deg.**	**min**			**Sampling rate (kHz)**	**Duty time/ period (min)**	**Sampling rate (kHz)**	**Duty time/period (min)**	
Anse-à-Valleau	64	32.244	49	5.464	11-24 July	43	10	continuous	250	2 min / 10 min	40
Cloridorme	64	49.916	49	11.606	13-24 July	56	10	continuous	250	2 min / 10 min	40
Percé	64	11.856	48	31.856	29 July to 24 August	48	10	continuous	250	continuous	40
Mal-Bay	64	11.223	48	36.245	29 July to 24 August	42	10	continuous	250	continuous	40

4.4.2 Sound emissions and CTDs

After installing the pair of circular hydrophone arrays on the seafloor at the monitoring sites, their precise location must be determined to refine the first overall location of the array center obtained by ranging interrogations of the VEMCO acoustic release attached to the center and get the exact positions of the 20 LF hydrophones and 4 HF hydrophones of the arrays.

These precise locations of all hydrophones of the arrays can be obtained by emitting sounds at a series of known positions (from GPS recorders) around the receiving hydrophone arrays. Then, the *tdoa*s of these sounds at the hydrophones are used to get the unknown positions of the array center and the hydrophone x,y coordinates, providing the two-dimensional shape (expectantly circular) and orientation of the arrays that is needed for determining the bearings of the targeted whale calls and other sources. This procedure is not presented here and will be described in detail in a future dedicated paper.

Among the emitted sounds, we have the noise emanating from the two working vessel propellers, a 16-s sequence of 5 NARW upcalls (see Parks et al. 2011) emitted by a Lubell VC2C transducer, discrete knocks on vessel hull, chirp signals from a Benthos sub-bottom profiler mounted on the R/V Coriolis II, and ship noise from distant transiting ships tracked using their AIS positions.

Specifically for assessing the hydrophones positions and arrays orientations, the small boat made a 360° circular trajectory at ~500 m radius around each array and emitted NARW upsweeps at equal intervals during the course (Table 4, Ring pattern). The vessel sailing at a speed of ~5 kn around the array simultaneously provided a LF broadband sound source from all azimuths.

Other series of sound emissions were produced on a transect perpendicular to the shoreline, at mid-distances from the two circular arrays, and 2 other transects parallel to shore (Appendix A, Figure 26, Table 4, perpendicular and parallel patterns). Since the R/V Coriolis II was equipped with a LF sub-bottom echo sounder, it was activated during the transects to provide sharp broadband transient sounds for localization. To get the inshore-offshore sound speed cross-section (Figure 28, Figure 27), CTD profiles over the water column were collected at a series of stations along the perpendicular transect using an SBE 19-plus CTD (Appendix A, Figure 26, Table 5).

The source level (SL) of emitted LF upsweep signals with the Lubell VC2C transducer is unknown but will be estimated from the received levels (RL) on the arrays and a transmission loss (TL) model. Experimental estimates of the detection ranges of the arrays for NARW upsweep calls will then be computed using the array PAM performance equations (Gervaise et al. 2019a, 2019b; Gervaise et al. 2021) and the SLs of the emitted upsweeps and published NARW upsweep SLs (Clark et al. 2011; Hatch et al. 2012).

4.4.3 Acoustic recordings

The acoustic data were recorded in two sets of files, one for the LF hydrophones with 20 channels, and one for the HF hydrophones with 4 channels. A proprietary Omnitech file format ('.oei') is used for data storage on the AR. Software is provided to convert the acoustic data to .wav format. A total of 320 hours of recording was obtained for the deployment of the pair of circular arrays in Honguedo strait, and 570 hours for the Mal-Bay—Percé site, for a total storage of 21 TB.

5. EXAMPLES OF RECORDED SOUNDS AND THEIR BEARINGS

5.1 Signal-to-noise ratio enhancement with beamforming

A series of 4 real NARW upsweep contact calls at ~ 4-s intervals embedded in dense and variable background noise were recorded on August 4 at Mal-Bay (Figure 12). While the noise on hydrophones 13, 15, 17 is relatively uniform, it includes strong impulses on channels 1, 3, 5, 7. Such variations of noise patterns among the hydrophones suggest a non uniform exposure of the array to some local bottom noise sources, preferentially affecting one side of the array. From the position of the hydrophones around the array (Figure 13) and the geographic location of the array (Figure 16) we note that hydrophones 1, 3, 5, 7 and hydrophones 11, 13, 15 are on opposite sides of the array. This suggests that the local mechanical noise is coming from the side where the array is connected to its lander and AR with the extra cable. Knocks from the array structure or friction with moving cable might be the source. However, the simple beamforming technique (known as delay and sum : i.e. maximum likelihood beamformer for each FFT frequency supposing a plane wave) successfully filtered out this interfering noise in other directions than our targeted source (Figure 13).

The maximal signal energy obtained the from beamforming goniogram over the [75 Hz and 225 Hz] band (Figure 13, inner polar plot line) indicates that the upsweep call was coming from the SE direction. This is clearly illustrated by the eight different beamformed spectrograms over the full 360° circle, where the best SNR is on the lower right corner spectrogram. On this example, the goniogram indicates significant energy (around 38 dB re 1 µPa rms) in the frequency band of interest that is spread over most directions (Figure 13, inner polar plot red dashed line circle), likely due to the above suggested close emission of impulsive structural noise arising from one side of the array. The energy in this same band in the call azimuth is 71 dB re 1 µPa rms, giving a beamforming enhanced SNR of 33 dB (71dB – 38 dB). This compares to a SNR of ~ 12 dB from single hydrophone measurements (Figure 12).

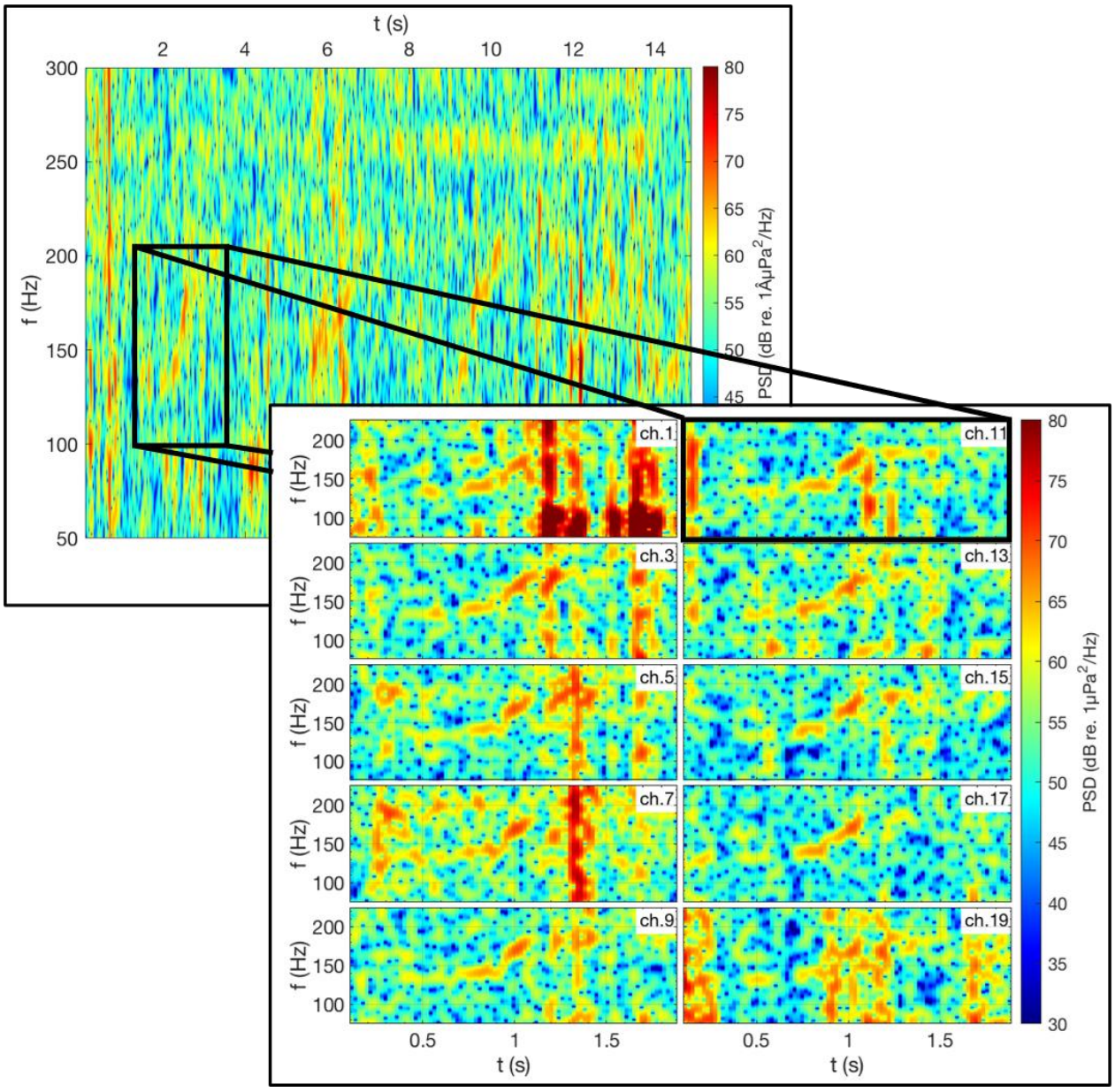

Figure 12. Spectrogram examples of the recordings of a NARW upsweep contact call from a distant whale by the Mal-Bay circular hydrophone array at 00:52:46 UTC on August 4.

Top: 15-s spectrogram between 50 Hz and 300 Hz from one of the 20 LF hydrophones of the array showing faint traces of NARW upsweep calls between 100 Hz and 200 Hz.

Bottom: 2-s zoomed spectrograms of one of the NARW upcalls as recorded by 10 hydrophones of the array.

N.B.: The time axis of the zoomed spectrogram is not referring to that of the top spectrogram.

The spectrogram has a resolution of 0.02 s × 4.9 Hz (FFT= 2048, Fs= 10000 sa/s, Kaiser window, overlap = 0.9, no padding).

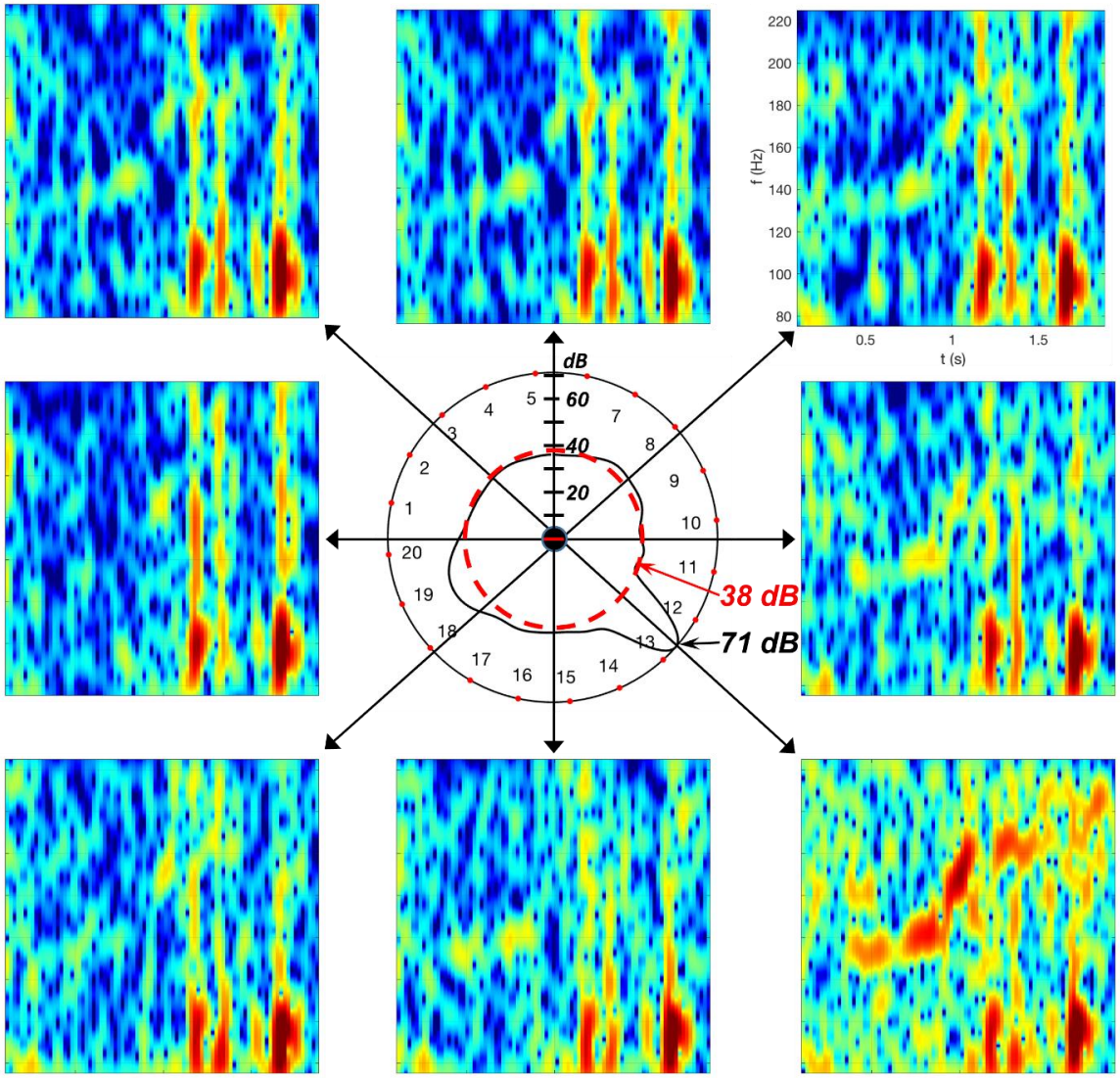

Figure 13. Examples of the application of the simple beamforming technique on Figure 12 NARW upsweep for 8 azimuths around the Mal-Bay circular hydrophone array at 00:52:46 UTC on August 4, showing 2-s [75 Hz and 225 Hz] spectrograms of recomposed signals in the indicated azimuth directions.
Spectrogram parameters as indicated for Figure 12. Goniogram resolution: 1°.
The presence of a NARW upsweep contact call from a distant whale arising from one direction (lower right) is enhanced from the SNR improvement of beamforming, compared to the individual spectrograms from the LF hydrophones of the array shown on Figure 12.
The shape in the center of the circle is the goniogram over the [75 Hz and 225 Hz] band, which indicates the relative signal energy in the targeted frequency band from all directions around the array. Hydrophone positions and numbers are associated with red dots along the circle.

The SNR enhancement of beamforming allows detecting (e.g., Figure 14, bottom panel) distant weak signals, hardly distinguishable from background noise (e.g., Figure 14, top panel), that would have otherwise been ignored. The incoherent background noise from different directions gets canceled due to destructive interference as explained in Section 1.2, Figure 1. The coherent signal coming from the direction 115º is enhanced by the summation over all hydrophones that accounts for the *tdoa*s for that azimuth. This upsweep call was not perceived on the hydrophones of both arrays, and the source location cannot be estimated by crossing the directions of arrivals. However, from the signal strength, and the transmission loss in the area (Gervaise et al. 2021), the source is thought to be at a range > 80 km. This hypothesis will be validated once the second method of source localisation, using single bearing estimates combined with transmission loss and SL estimates, will be implemented.

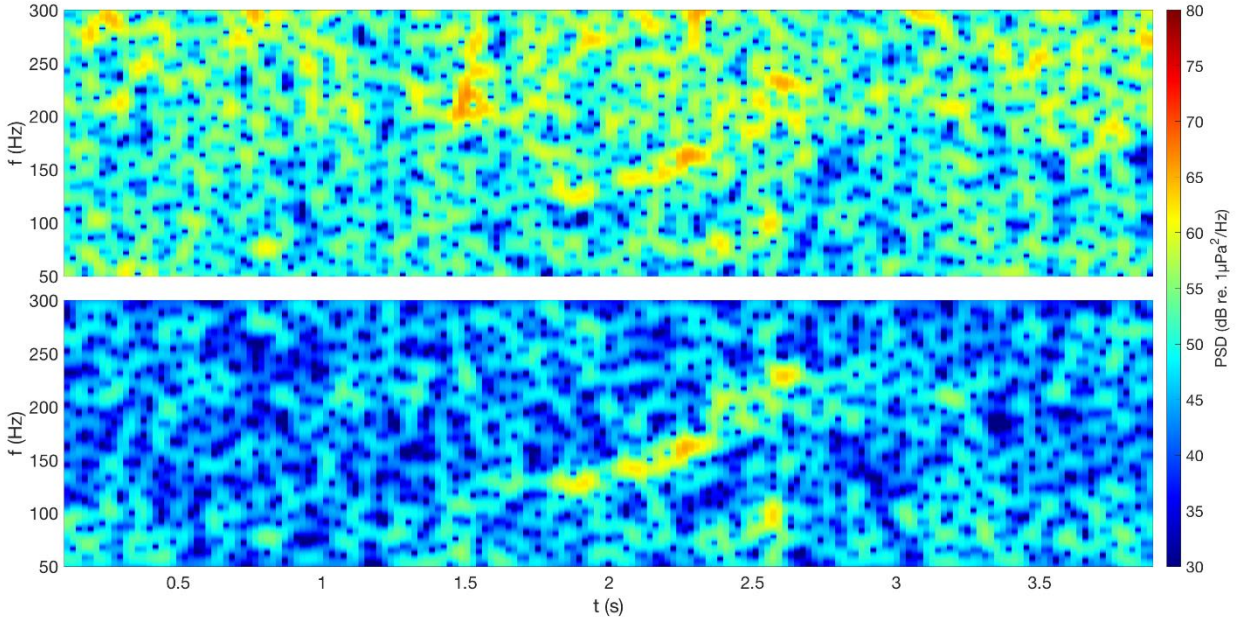

Figure 14. Comparison between a single hydrophone spectrogram (top panel) versus a spectrogram of reconstructed signal in the source direction (115º) from simple beamforming, pointing towards a weak and distant NARW upcall (bottom panel) recorded at 02:58:11 UTC on August 4.
Spectrogram parameters as indicated for Figure 12.

Other frequent low-frequency mysticete calls, overlapping with the frequency band of the NARW upsweep calls, were recorded during the field experiments with the arrays off the Gaspé peninsula (e.g., Figure 15). When they co-occur with NARW upsweep contact calls, there is a risk to degrade the beamforming SNR improvement of the NARW upsweep call, if these other sources are in the same azimuth as the calling NARW. One the other hand, the sharing of the same frequency band offers the possibility to locate other species while processing the array data in this band. Among the whale species sharing the NARW calling frequency band, we have humpback, minke, and sei whales.

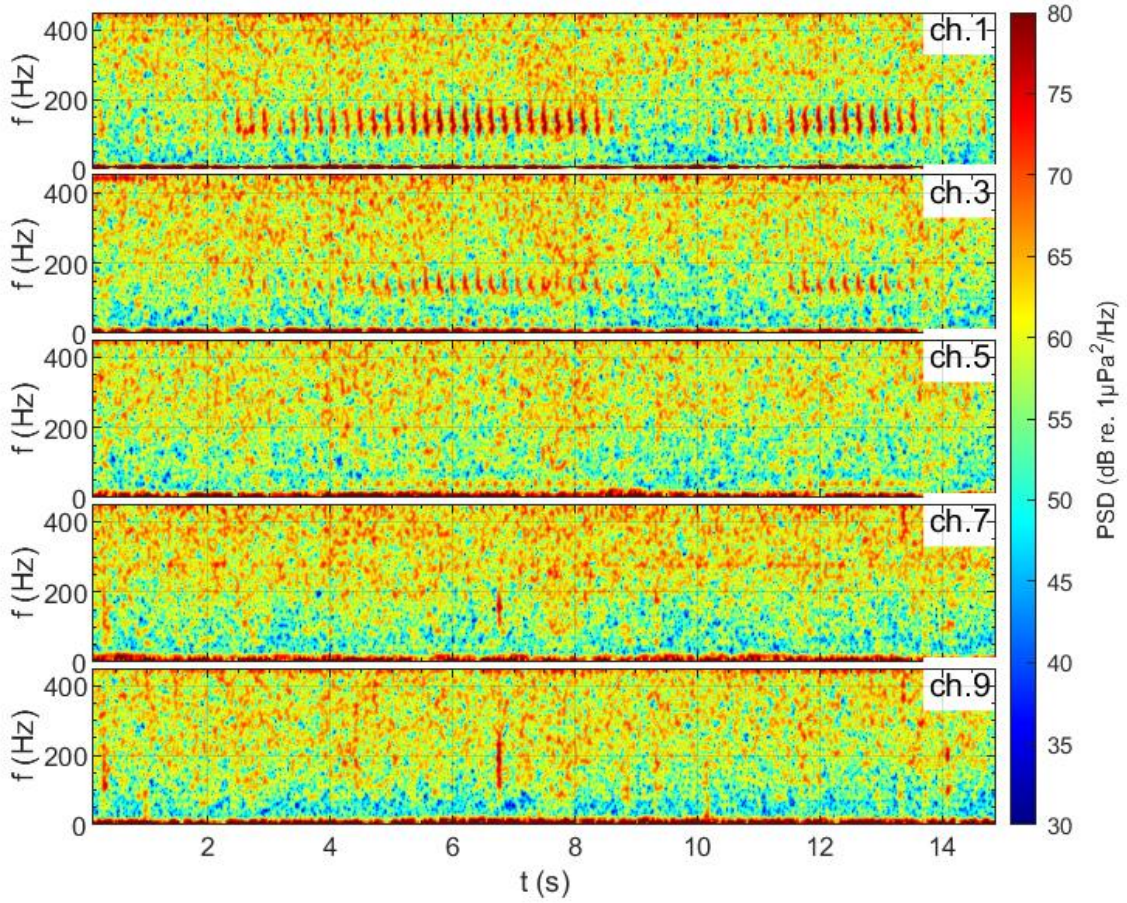

Figure 15. Spectrogram examples of a minke whale drumming sound, between 100 and 200 Hz on channels 1 and 3, recorded at Anse-à-Valleau from 5 hydrophones of the circular array at 04:33:08 UTC on July 14.
Spectrogram parameters as indicated for Figure 12.

5.2 **Binaural source detections and beam-crossing localization**

When the signal of interest is present on both arrays of the WBR pair, the source location is at the intersection of the two lines corresponding to the two azimuths to the source. An example is provided for a NARW upsweep call at ~ 20 km from the coast in northern Shediac through (Figure 16).

That strong NARW upsweep call (Figure 16, first call on top panels, azimuth 126°) was followed by another faint call (t ≈ [2.5 to 3.5 s], red box (a)) from a more southern azimuth (135 °) to the Mal-Bay (MLB) array (Figure 16). This second call was not clearly detected on the Percé (PRC) array hydrophones, most likely because the obstruction of Bonaventure Island prevented the detection of sources located in the angular sector further south. If we assume that this second call was from another whale (*w2*) responding to the first caller (*w1*) located at x_{w1} (Figure 17, red dot), we can estimate the location of that second whale, x_{w2} (Figure 17, green dot and line segment), using the single bearing estimated from Mal-Bay array combined with additional information.

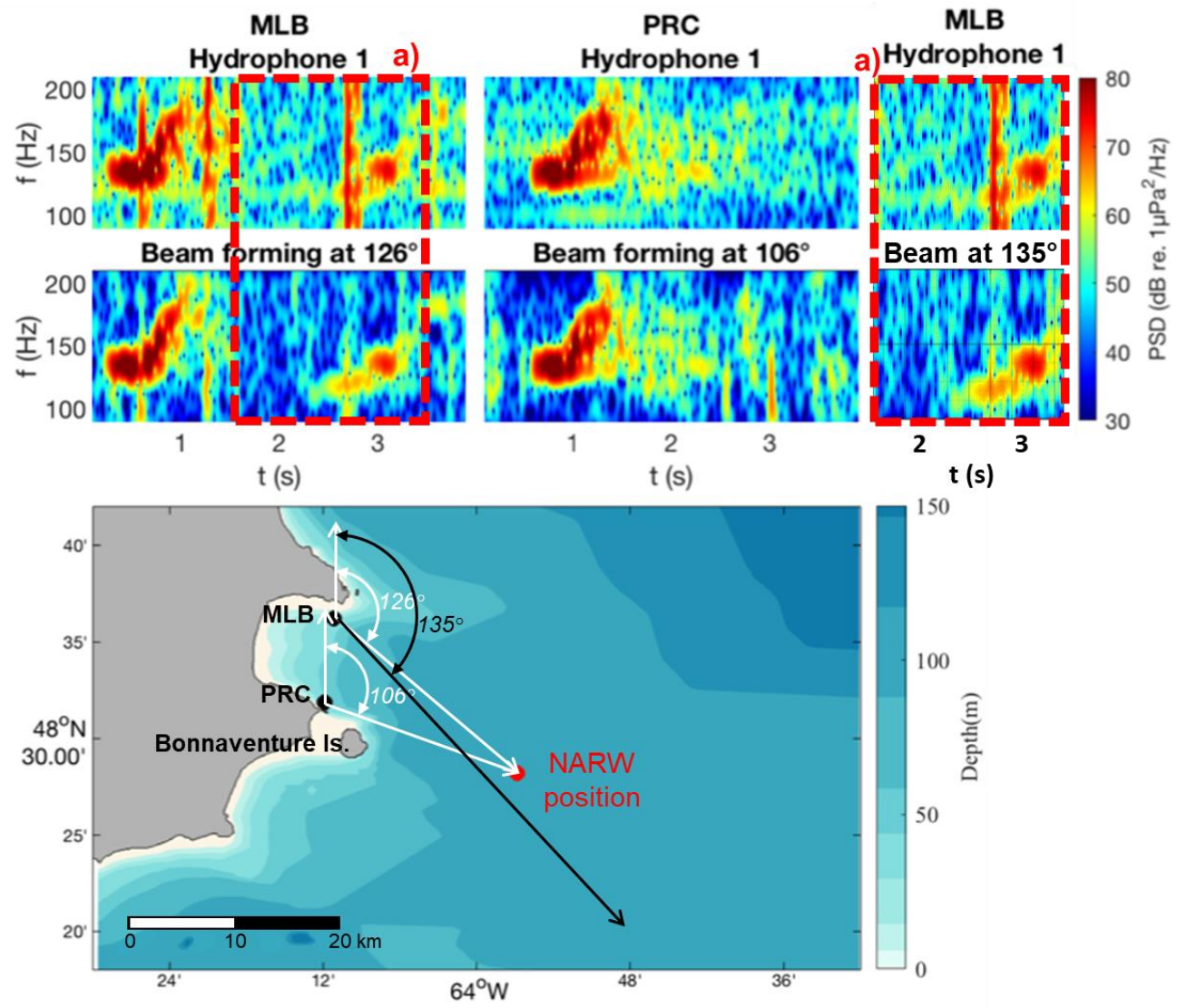

Figure 16. Map of the estimated position of a NARW upsweep call in northern Shediac through, from the crossing of the two bearings estimated by simple beamforming for the two circular hydrophone arrays at Mal-Bay (MLB) and Percé (PRC) (Lower panel).
Spectrogram parameters as indicated for Figure 12.
Upper panels: 4-s spectrograms from received levels at the hydrophone 1 of the arrays at Mal-Bay (left) and Percé (center), with 2-s extract (a) (red dashed line box) for Mal-Bay second upsweep call (right).
Middle panels: 4-s spectrograms of beamformed received levels in the source directions at Mal-Bay (left) and Percé (center), with 2-s extract for Mal-Bay second upsweep call (right).

The observed time interval *tdoa* of about 2.3 s between the two calls, is the sum of the elapsed time between the emissions and the difference of propagation times from the two sources to the receiving array:

$$tdoa = \frac{D(x_{w1},x_{w2})}{c} + \delta t + (r_{w2} - r_{w1})/c, \quad (1)$$

where ($D(x_{w1},x_{w2})$ is the distance between the two whales, c is the average water column sound speed, δt is the response delay of $w2$ after receiving the signal from $w1$, and r_{w2} and r_{w1} are their respective ranges.

Based on an average water column sound speed of ~ 1470 m s^{-1} and assuming a quasi-immediate response (δt = 0.3 to 1 s), x_{w2} can be estimated on the azimuth 135° from MLB site as the set of points satisfying equation (1).

This gives a range of positions for $w2$ that is at the southern limit of the angular detection sector of the Percé array because Bonaventure Island is blocking the sources located further south (Figure 17, yellow line).

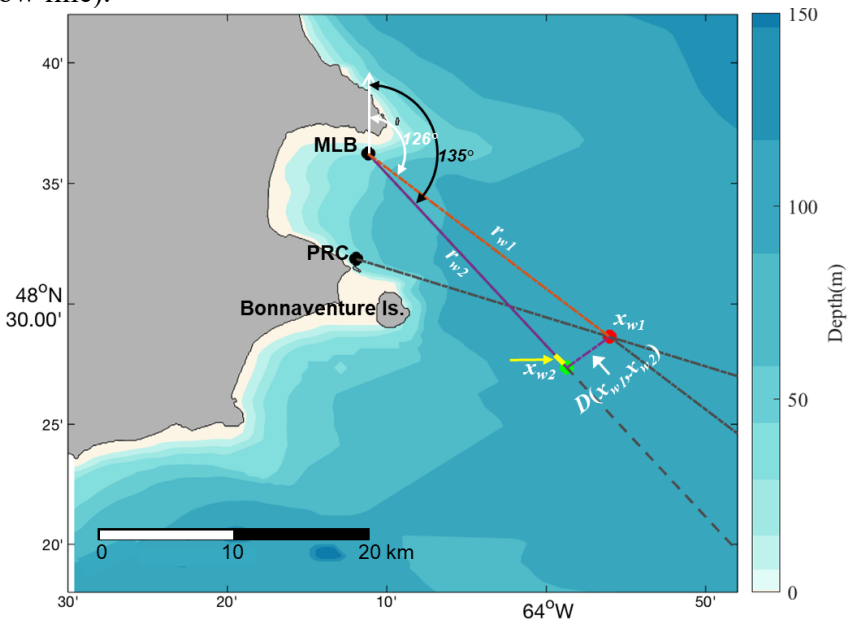

Figure 17. Map of the estimated position of a second NARW upsweep call in northern Shediac through that occurred ~2.3 s after the one positioned in Figure 16, which might origin from a responding whale.
Here, the localization is done using the single bearing available, combined with the estimated distance of the responding whale along this azimuth to Mal-Bay array and considering the ~2.3 s time interval between the two calls (see text).

An example of a real upsweep call from a NARW cruising in Honguedo strait, about 45 km offshore (estimated from the TL method), illustrates the beamforming capacity for extracting targeted signals that are deeply sunk in background noise (Figure 18). This call was manually detected by an expert with high-resolution spectrograms from the 20 hydrophones of the array. The repetition of the barely detectable event on all hydrophones of the array allowed the expert to distinguish the faint signal from the ambient noise.

Other whale localization examples from the bearing crossing method are provided for blue whale D-call in the ~ [90 – 40 Hz] band detected by the two arrays in the Honguedo strait (Figure 19, Figure 20). Strong D-calls were detected at ~ 15 km off the coast, in front of the array located at Anse-à-Valleau on 16 July (Figure 19). Weaker calls were detected at a ~50 km offshore a few days before (Figure 20).

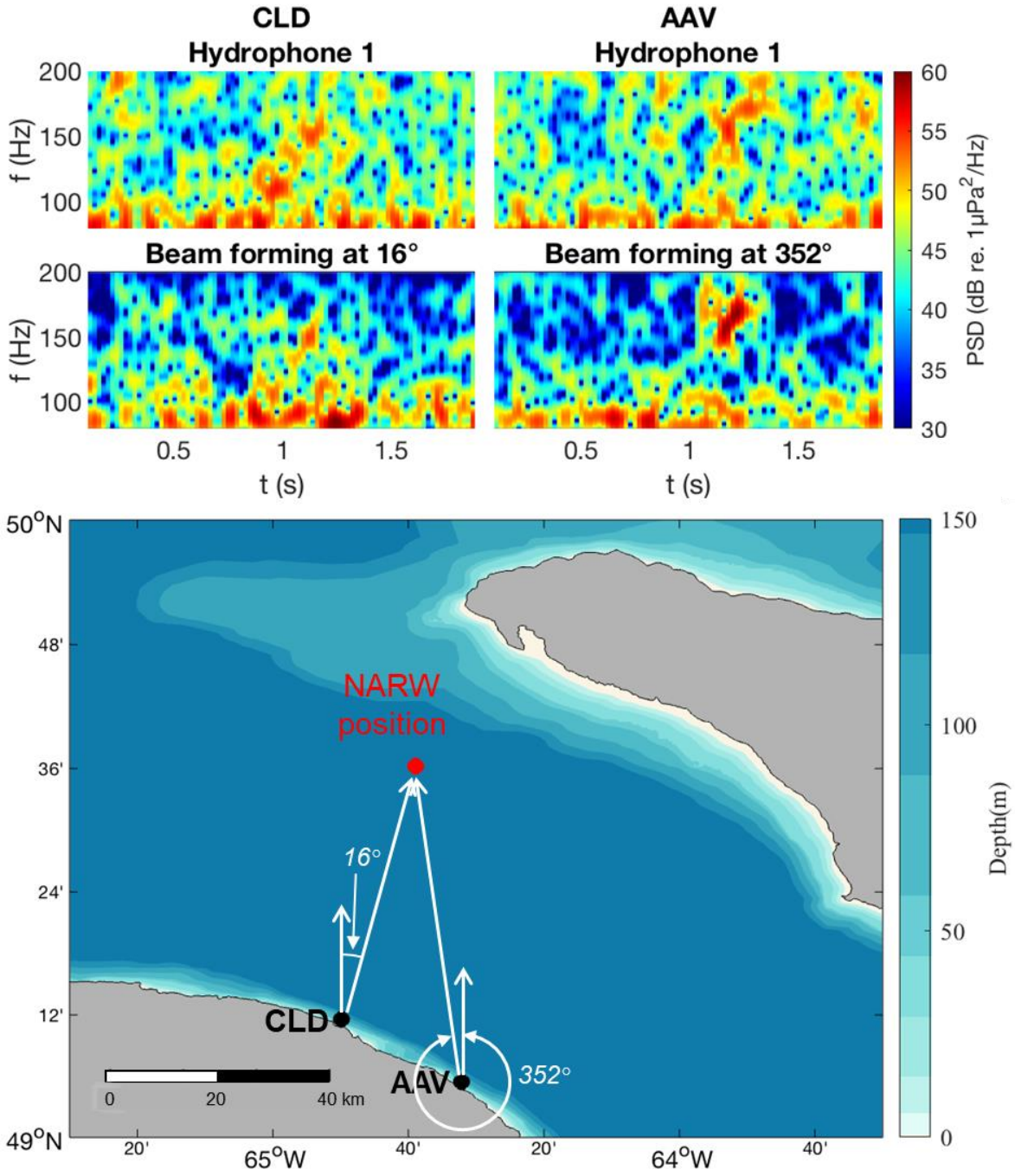

Figure 18. Map of the estimated position of a faint NARW upsweep call in Honguedo strait, on 16 July 2021 19:03 UTC, from the crossing of the two bearings estimated by simple beamforming for the two circular hydrophone arrays at Cloridorme (CLD) and Anse-à-Valleau (AAV) (Lower panel).
Spectrogram parameters as indicated for Figure 12.
Upper panels: 2-s spectrograms from received levels at the hydrophones 1 of the arrays at Cloridorme (left) and Anse-à-Valleau (right).
Middle panels: 2-s spectrograms of beamformed received levels in the source direction at at Cloridorme (left) and Anse-à-Valleau (right).

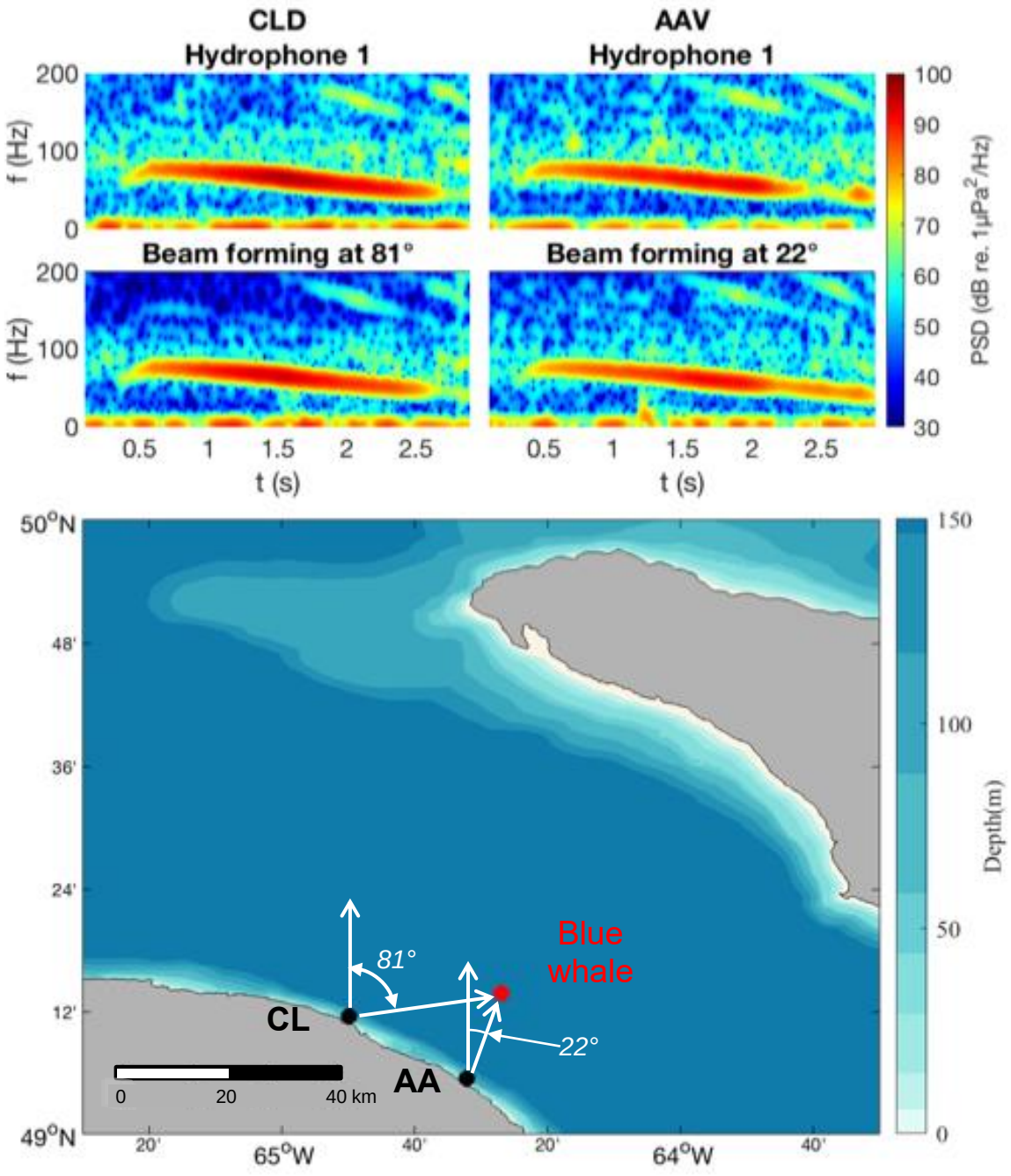

Figure 19. Map of the estimated position of a blue whale D call of in northern Honguedo Strait, on 15 July 09:50 UTC, from the crossing of the two bearings estimated by simple beamforming for the two circular hydrophone arrays at Cloridorme (CLD) and Anse-à-Valleau (AAV) (Lower panel).
Spectrogram parameters as indicated for Figure 12.
Upper panels: 3-s spectrograms from received levels at the hydrophones 1 of the arrays at Cloridorme (left) and Anse-à-Valleau (right).
Middle panels: 3-s spectrograms of beamformed received levels in the source direction at Cloridorme (left) and Anse-à-Valleau (right).

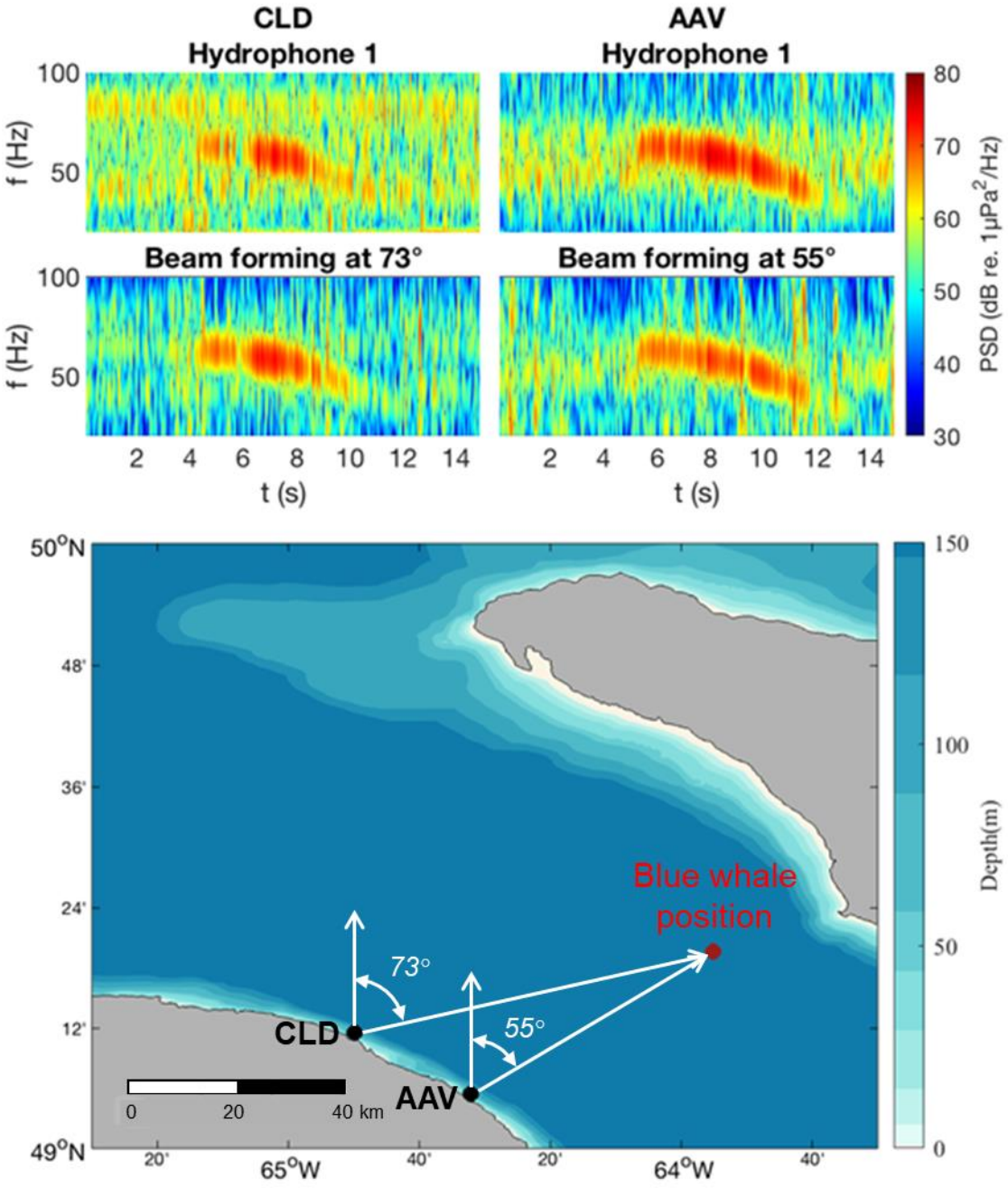

Figure 20. Map of the estimated position of a blue whale D call in northern Honguedo Strait, on 13 July 23:46:04 UTC, from the crossing of the two bearings estimated by simple beamforming for the two circular hydrophone arrays at Cloridorme and Anse-à-Valleau (Lower panel).
Spectrogram parameters as indicated for Figure 12.
Upper panels: 14-s spectrograms from received levels at the hydrophones 1 of the arrays at Cloridorme (left) and Anse-à-Valleau (right).
Middle panels: 14-s spectrograms of beamformed received levels in the source direction at Cloridorme (left) and Anse-à-Valleau (right).

5.3 **Tracking a moving source: example with a transiting AIS-positioned ship**

The trajectory of ships transiting in the hydrophone array detection areas can be easily obtained from the crossing of the azimuths of their radiated noise received at the array pairs. If the position of the ship is known, from the AIS broadcasted position or other positioning systems, it is then possible to compare with the estimated position from the beam crossing. This approach was used to determine the relative positions of the hydrophones of the arrays after their deployments, and verify if the circular shape of the array was maintained during deployment. This method will be presented in a dedicated publication.

This pair of bi-static (emission and reception at different locations) acoustic systems provide information about the underwater propagation in the study area that can be exploited to assess the performance of the arrays and the characteristics of radiated noise by the ship. Using this information is beyond the scope of the present report. However, an example of the available information is illustrated below for a merchant ship transiting in the Mal-Bay Percé area (Figure 21).

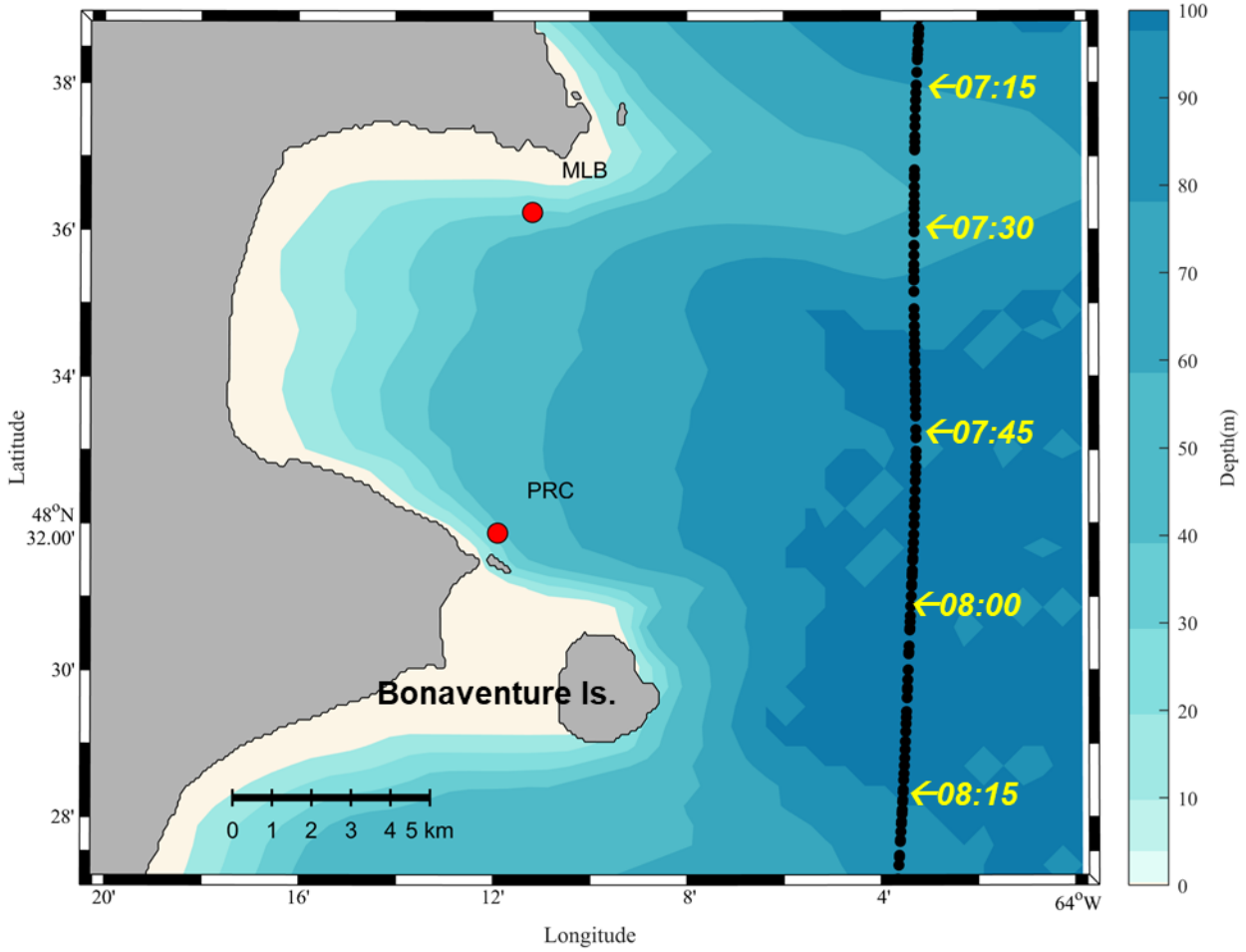

Figure 21. Trajectory of a transiting merchant ship heading south in the detection area of the Mal-Bay and Percé hydrophone array pair on 17 August between 7:10 and 8:20 UTC.

The radiated noise from the southward transiting ship is continuous and covers the LF band below 450 Hz on both Mal-Bay and Percé arrays, only after the ship has passed the shoaling topography after ~07:30 UTC (Figure 21, Figure 22). On Mal-Bay array, this strong broadband noise level goes on up to the end of the time segment at 08:20. At Percé array, its level drops at ~8:02 (Figure 22 bottom panel), when the ship azimuth exceeds ~ 120° and the ship line-of-sight is blocked by Bonaventure Island (Figure 21, Figure 23 bottom panel). This pattern illustrates the blinder effect of the embayment between Mal-Bay and Percé and of the underwater topography in determining the effective detection area of the hydrophone arrays. The presence of another distant ship transiting with another trajectory appears on the azigrams before 07:30 (Figure 23).

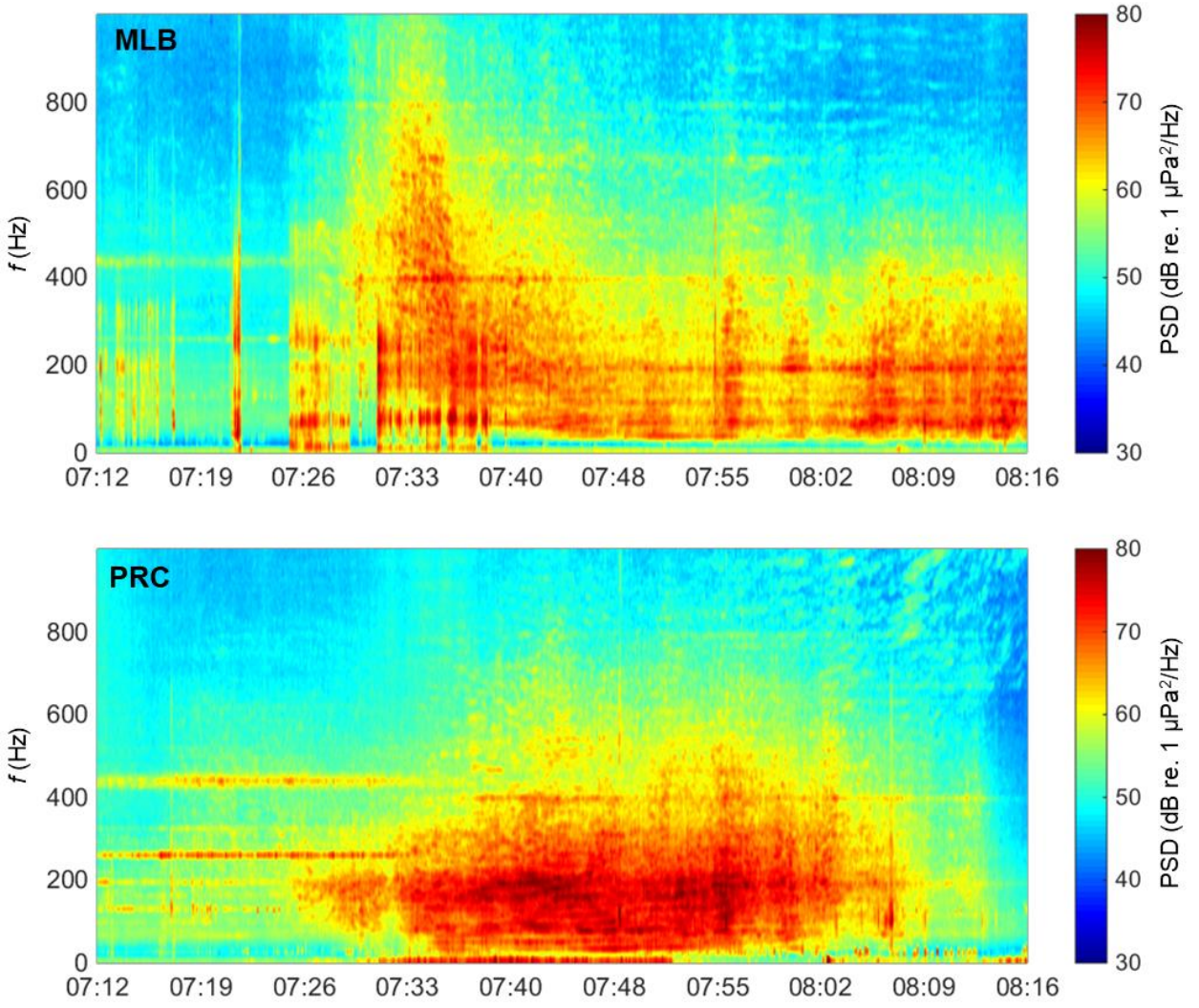

Figure 22. Spectrograms of the [0-1 kHz] recordings from single hydrophones (#1) at the Mal-Bay (upper panel) and Percé (bottom panel) arrays during the transit of the merchant ship heading south along the trajectory displayed in Figure 21 on 17 August between 7:12 and 8:16 UTC.
Spectrogram parameters as indicated for Figure 12.

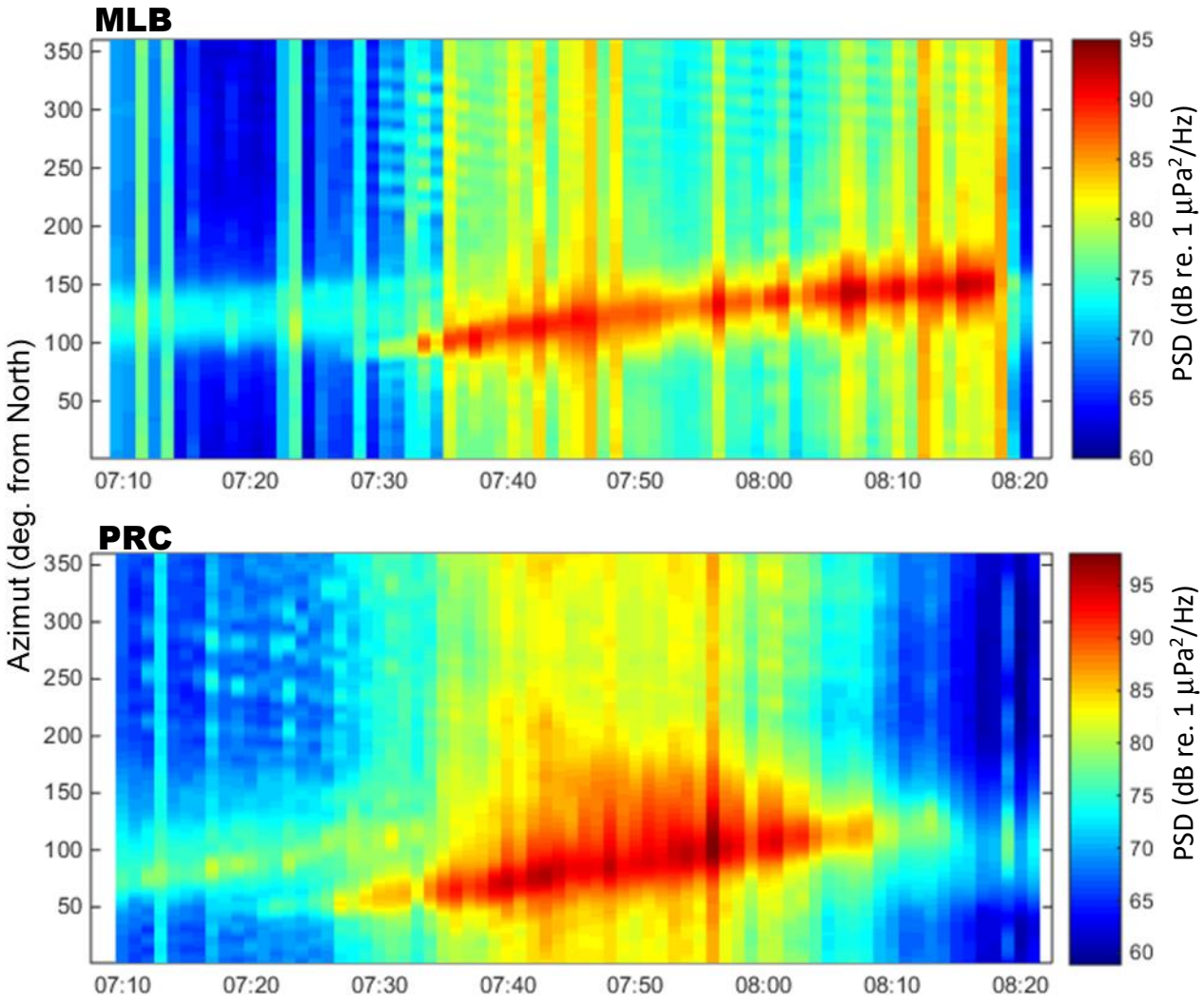

Figure 23. Azigrams of the [50 - 300 Hz] beamformed broadband acoustic energy at the Mal-Bay (MLB) (upper panel) and Percé (PRC) (bottom panel) arrays during the transit of the merchant ship heading south along the trajectory displayed in Figure 21 on 17 August between 7:10 and 8:20 UTC.
Spectrogram parameters as indicated for Figure 12. Simple beamforming with 1° resolution.

6. DISCUSSION

The work presented in this report is derived from previous studies on the comparison of the performance of various PAM systems to monitor NARW in real-time in the Gulf of St. Lawrence. It is the first field trial of the implementation of the optimal PAM system as described by the simulation studies of Gervaise et al. (2019a, 2019b; 2021). To our knowledge, it is the first time such pairs of large-size circular hydrophone arrays, deployed at short distances from favorable coastal sites, have been used to detect and localize LF calls of baleen whales. The preliminary results of this experiment illustrated in this report, conform with the predictions of the simulation studies. The analysis of the whole dataset collected during the experiment will be presented in further publications.

The beamforming capacity of these directional hydrophone antennae significantly enhances the SNR of targeted acoustic events, by amplifying the signal of interest and cancelling noise arising from sources in different directions. This property offers the advantages of:

- expanding the detection range of traditional omnidirectional or directional (e.g.,Thode et al. 2012) PAM systems,
- reconstructing the signal in the source direction for easing its detection by time-frequency-based algorithms,
- finding the source location by a) the crossing of the bearings from 2 arrays located at different locations or by b) combining the bearing from a single array with information from the SL of the target call and the transmission loss field in the study area.

The use of such high-performance PAM systems opens the access to new information on the *in situ* behavior of targeted whales in their environments. This information can become available in real time when the systems are cabled to an on-shore control and processing station, for example for monitoring critical areas where shipping noise severely limits the capabilities of usual PAM systems. The next step of this DFO research project will aim address this, to track LF calling whales in their habitat in GSL, which is crossed by a medium traffic seaway.

6.1 Mooring challenges

Aside from the challenges associated with long preparation time and the complicated logistics, the realization of the field work required planning within the constraints of weather, waves, tides, and currents. In addition, the technology used was new and the large structure of the arrays presented a handling challenge. Despite careful planning and a test in shallow depths off DFO/MLI site, the reality of field work required imagination and flexibility from the technical team.

The complexity of deployment and retrieval of the moorings called for low wind and small wave heights. Weather was therefore a concern, although we were lucky to find calm weather windows at suitable times during the field trials. Temporarily sinking the assembled arrays near the mounting beach through deflating the floatation tube (and attaching them to a nearby dock in 3

of the 4 cases), the apparatus could remain in standby while waiting for proper conditions (ship availability, weather, daylight, tides). The use of inflatable tubing proved to be an essential element of the mooring process.

The flexibility of the I-beam and the drag of the structure did not allow to tow the structure at speeds faster than 1-2 kn. Higher speeds resulted in the sinking and bending of the structure. This was particularly an issue for the two sites on the Honguedo strait, where the towing was against the Gaspé Current flowing at approximatively the same velocity (Benoit et al. 1985; Galbraith et al. 2020, Fig. 59). Thus, reaching the research vessel from the array mounting site on the beach was longer than expected. At some point, we were barely able to stay on the same location to prevent this bending of the array. Towing the structure when rising tide slowed the downstream flowing surface current or at slack waters did help. A tow line has been added through the course of the process to tow the circular structure from one central point (Figure 6, purple line) rather than from a V-line that tended to force the structure to fold on itself in a sandwich.

The lowering of the array to the seafloor was also more complicated than anticipated. Some volume of air stayed trapped in the inflatable tube at the lander side because of the outflow constriction in the two supply/exhaust hoses and, as a result, the unbalanced outflow resistance between the two hoses amplified the non-uniform sinking of the array structure (cf. Figure 6). The array floated for many minutes without sinking. A procedure that allowed to avoid this effect was to lower the lander in the water before opening the valve to force the air exhaust when it is opened. In future operations, a vacuum pump will be used to rapidly drain all the air contained in the green inflatable tube under the array structure.

Another factor that did not help to properly lower the structure is the attachment setup of the lowering cables. On each half of the circle, five ropes of specific lengths forming the bridles are attached from the structure to a master point. A lowering line from each master point goes to each of the two vessels. When the angle formed by the lowering line and the plane of the array structure is not 90º, the tension is higher on the two outers of the five lines, which leads to bending of the flexible array structure towards its center. Moreover, this setup leads to strong tension on the structure when the distance between boats varies, which is prone to bend, twist or flip the structure upside down. A better approach will be to attach equal lines from the structure to a master point located over the center of the structure. Thus, the structure would maintain a circular shape and orientation by gravity. This would also prevent the structure from sinking faster from one side as above discussed.

6.2 **Array circular frame**

Although the arrays were framed with stiff fiberglass I-beams, the relatively large size of the structure caused enough stress to deform the ring during towing and mooring operations. When towing with a V-line, the tension in the bridle outer lines forced the circular array to sink in its middle axis while the outer attachment points on both sides tended to stay at water level. Thus, the structure wanted to bend in a “taco” shape. A more hydrodynamic shape in the front of the structure along the towing axis or more floatability would help to move it along during the towing.

The role of the radial tension cables on the array structure was to prevent its stretching in an oval shape. However, this system did not prevent some sections of the structure to fold-in towards the center of the array during the towing and lowering operations, as it was observed in the deployment at Anse-à-Valleau. The post-processing localization of the array hydrophones at Cloridorme site showed that the array adopted an eight-shaped figure on the seafloor. To prevent such deformation of the flexible array structure during the operations, its fiberglass I-beams will be thickened in the next version of the array structure (Figure 24). Moreover, a master single lowering point, located over the center of the structure, to which both vessels will be linked will also prevent this folding trend due to non-uniform lateral tensions (Figure 25).

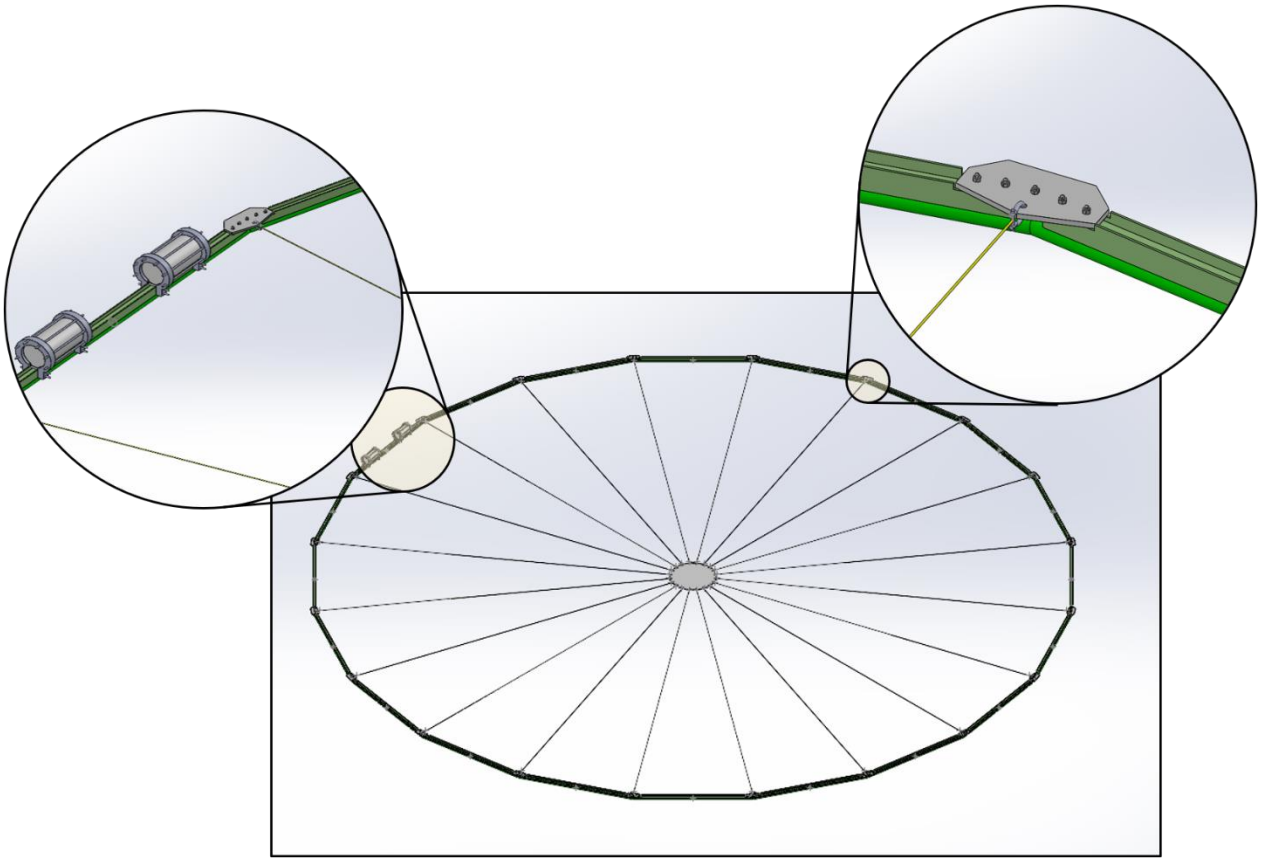

Figure 24. Sketch of the re-enforced fiberglass I-beam circular frame of the array with mounted electronic casings for cable deployments to shore, for powering the array, and transferring the commands and data to a coastal station through a fiber optic Ethernet connection.

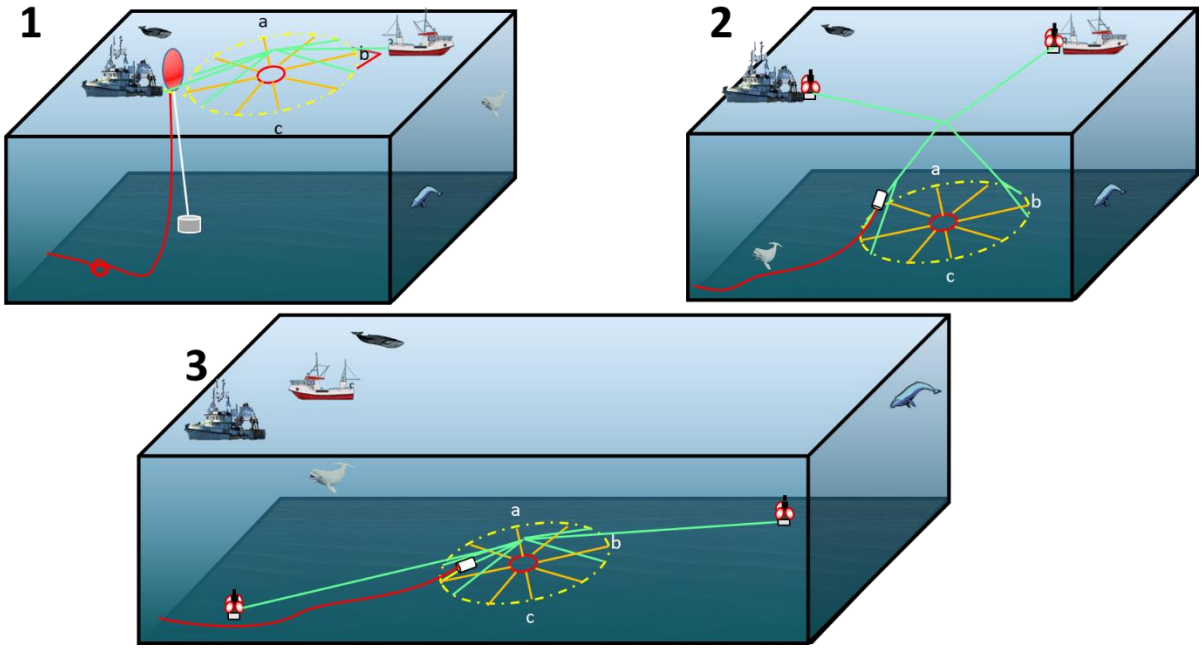

Figure 25. Mooring steps of the circular hydrophone array from a single central attachment.

1. Connection of the towed circular array to the previously deployed electro-optical cable.
2. Lowering of the circular array suspended from a central single point by two coordinated vessels.
3. Deployment of the ground ropes for retrieving the arrays with their floats, anchors, and acoustic release systems at their ends.

7. PERSPECTIVES FOR FUTURE DEVELOPMENTS

The data collected during the summer of 2021 will be analyzed and used to test our detection and localization tools. This should bring us into phase II of the B-Rings project, with the implementation of a long-term installation connected to coast for power supply and data transmission in real time. Design options are examined, including the use of fiber optics to avoid signal loss over long distances, since the locations of the future networks would be up to 1 mile from the coast.

It is planned to process the data automatically at reception at a coastal base, then transmit the detection and localization results to the web by cellular communication. As mentioned in Section 1.1, the technology and infrastructure for this type of real-time processing is already in place for NARW detection on the Viking buoys in the Gulf of St. Lawrence.

ACKNOWLEDGMENTS

We would like to thank all the people, from various DFO regions and Directions who have contributed to make this work a success. The continuous assistance and ideas for the designs of mooring assemblies from the DFO/MLI DAISS oceanography team has been precious. The field work was particularly difficult to carry out, because of the shortage of CCG research ships and the absence of alternative vessels during a call for tenders. CCG helicopters were briefly considered as an alternative option for the mooring approach. The contribution of Monique Goit, DFO/HQ, and Randy King, DFO/MAR, were salvific to finally find a solution with a chartered vessel. The ensuing rescheduling of the accommodation reservations in the Gaspé peninsula, during the peak tourist season, with a demand boosted up by the context of the Covid 19 confinement, was a nightmare. The last-minute changes for the reservations of boats, trucks, and staff, was a constant headache throughout the summer. We are grateful to the crew of the R/V Coriolis II for their support during the mooring of the systems, and to the crews of the fishing vessels Virginia Audrey and Renaissance 93 for their help and quick response to our requests. We also acknowledge the contribution of Stéphane Bouchard for his clever piloting of our CCG outboard vessel. This work was supported by Fisheries and Oceans Canada. We are grateful to Samuel Giard (DFO, MLI) and Stéphane Blouin (Defence R&D Canada) for reviewing the manuscript and to Jaclyn Hill for her editorial work.

REFERENCES

Benoit, J., El-Sabh, M.I., and Tang, C.L. 1985. Structure and seasonal characteristics of the Gaspe Current. J. Geophys. Res.: Oceans **90**(C2): 3225-3236. doi:https://doi.org/10.1029/JC090iC02p03225.

Bourque, L., Wimmer, T., Lair, S., Jones, M., and Daoust, P.-Y. 2020. Incident report: North Atlantic right whale mortality event in Eastern Canada, 2019. Collaborative Report Produced by: Canadian Wildlife Health Cooperative and Marine Animal Response Society.

Clark, C., Ellison, W., Hatch, L., Merrick, R., Van Parijs, S., and Wiley, D. 2011. An ocean observing system for large-scale monitoring and mapping of noise throughout the Stellwagen Bank National Marine Sanctuary. Reports to the National Oceanographic Partnership Program, Stellwagen project.: 11pp.

Clark, C., Ellison, W.T., Southall, B.L., Hatch, L., Van Parijs, S., Frankel, A.S., and Ponirakis, D. 2009. Acoustic masking in marine ecosystems: intuitions, analysis, and implication. Mar. Ecol. Prog. Ser. **395**: 201-222.

Daoust, P.-Y., Couture, E.L., Wimmer, T., and Bourque, L. 2017. Incident Report: North Atlantic right whale mortality event in the Gulf of St. Lawrence, 2017. Collaborative Report Produced by: Canadian Wildlife Health Cooperative and Marine Animal Response Society, and Fisheries and Oceans Canada.

Galbraith, P.S., Chassé, J., Shaw, J.-L., Dumas, J., Caverhill, C., Lefaivre, D., and Lafleur, C. 2020. Physical Oceanographic Conditions in the Gulf of St. Lawrence during 2019. Can. Sci. Advis. Sec. Res. Doc. Fisheries and Oceans Canada: iv + 84 p. Available from https://waves-vagues.dfo-mpo.gc.ca/Library/40980856.pdf.

Gervaise, C., Simard, Y., Aulanier, F., and Roy, N. 2019a. Optimal passive acoustic systems for real-time detection and localization of North Atlantic right whales in their feeding ground

off Gaspé in the Gulf of St. Lawrence. Can. Tech. Rep. Fish. Aquat. Sci. Fisheries and Oceans Canada, Ottawa: ix + 58 pp. Available from http://waves-vagues.dfo-mpo.gc.ca/Library/40830020.pdf.

Gervaise, C., Simard, Y., Aulanier, F., and Roy, N. 2019b. Performance study of passive acoustic systems for detecting North Atlantic right whales in seaways: the Honguedo strait in the Gulf of St. Lawrence. Can. Tech. Rep. Fish. Aquat. Sci. Fisheries and Oceans Canada, Ottawa: ix + 53 pp. Available from http://waves-vagues.dfo-mpo.gc.ca/Library/40829613.pdf.

Gervaise, C., Simard, Y., Aulanier, F., and Roy, N. 2021. Optimizing passive acoustic systems for marine mammal detection and localization: Application to real-time monitoring north Atlantic right whales in Gulf of St. Lawrence. Applied Acoustics **178**: 107949. doi:https://doi.org/10.1016/j.apacoust.2021.107949.

Hatch, L., Clark, C., Merrick, R., Van Parijs, S., Ponirakis, D., Schwehr, K., Thompson, M., and Wiley, D. 2008. Characterizing the relative contributions of large vessels to total ocean noise fields: A case study using the Gerry E. studds stellwagen bank national marine sanctuary. Environ. Manage. **42**(5): 735-752. doi:https://doi.org/10.1007/s00267-008-9169-4.

Hatch, L.T., Clark, C.W., Van Parijs, S.M., Frankel, A.S., and Ponirakis, D.W. 2012. Quantifying loss of acoustic communication space for right whales in and around a U.S. National Marine Sanctuary. Conserv. Biol. doi:10.1111/j.1523-1739.2012.01908.x.

Parks, S.E., and Tyack, P.L. 2005. Sound production by North Atlantic right whales (*Eubalaena glacialis)* in surface active groups. J. Acoust. Soc. Am. **117**(5): 3297-3306. doi:https://doi.org/10.1121/1.1882946.

Pettis, H.M., Pace, R.M.I., and Hamilton, P.K. 2021. North Atlantic Right Whale Consortium 2020 annual report card. Report to the North Atlantic Right Whale Consortium.

Simard, Y., Roy, N., Gervaise, C., and Giard, S. 2016. Analysis and modeling of 255 source levels of merchant ships from an acoustic observatory along St. Lawrence Seaway. J. Acoust. Soc. Am. **140**(3): 2002-2018. doi:http://dx.doi.org/10.1121/1.4962557.

Thode, A.M., Kim, K.H., Blackwell, S.B., Charles R. Greene, J., Nations, C.S., McDonald, T.L., and Macrander, A.M. 2012. Automated detection and localization of bowhead whale sounds in the presence of seismic airgun surveys. J. Acoust. Soc. Am. **131**(5): 3726-3747. doi:https://doi.org/10.1121/1.3699247.

APPENDIX A

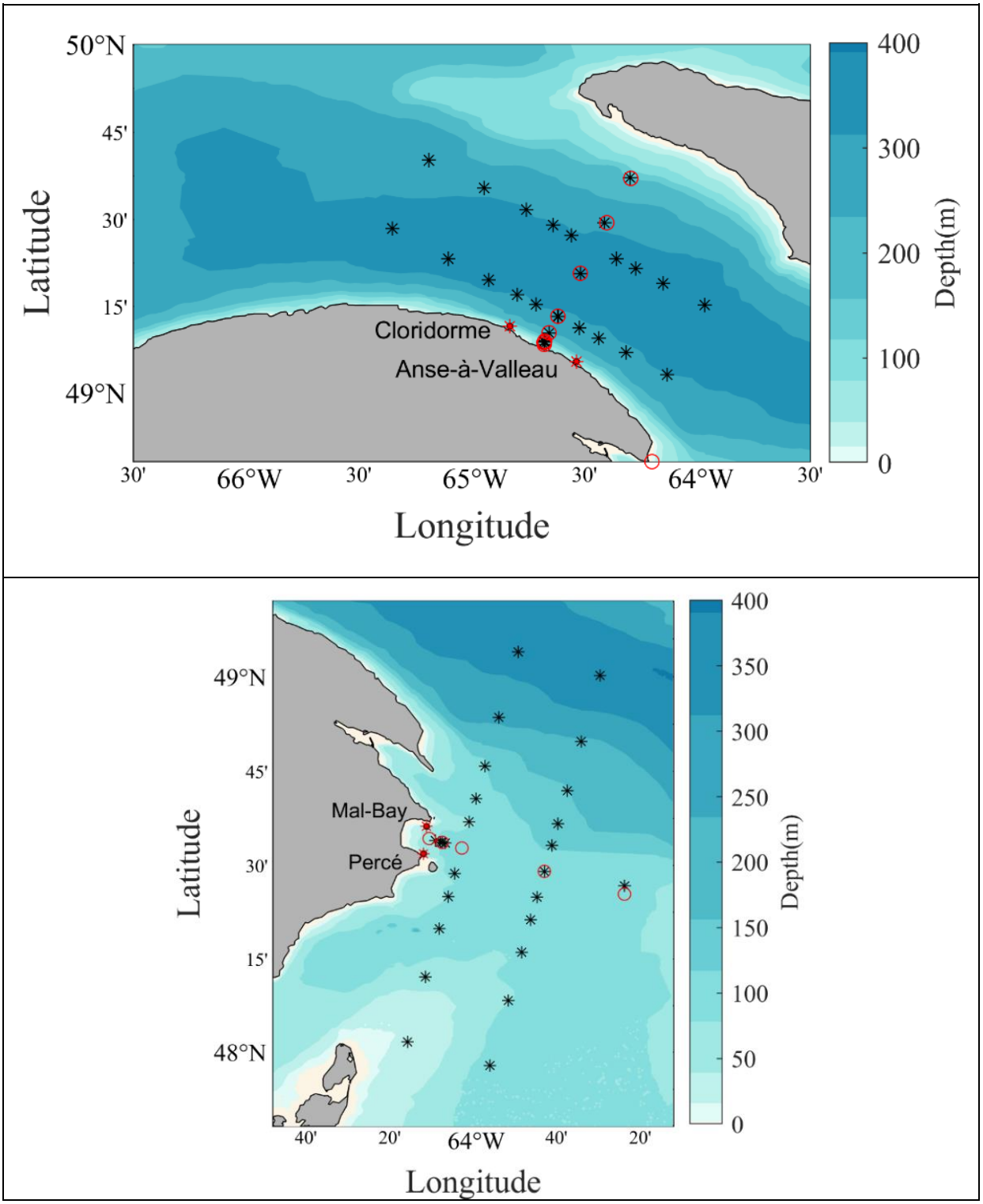

Figure 26. Maps of hydrophone array sites (red stars), ping emissions (black stars), and CTD (red circles) stations after the deployments of the circular hydrophone array pairs in Honguedo (top panel) and Gaspé regions (bottom panel).

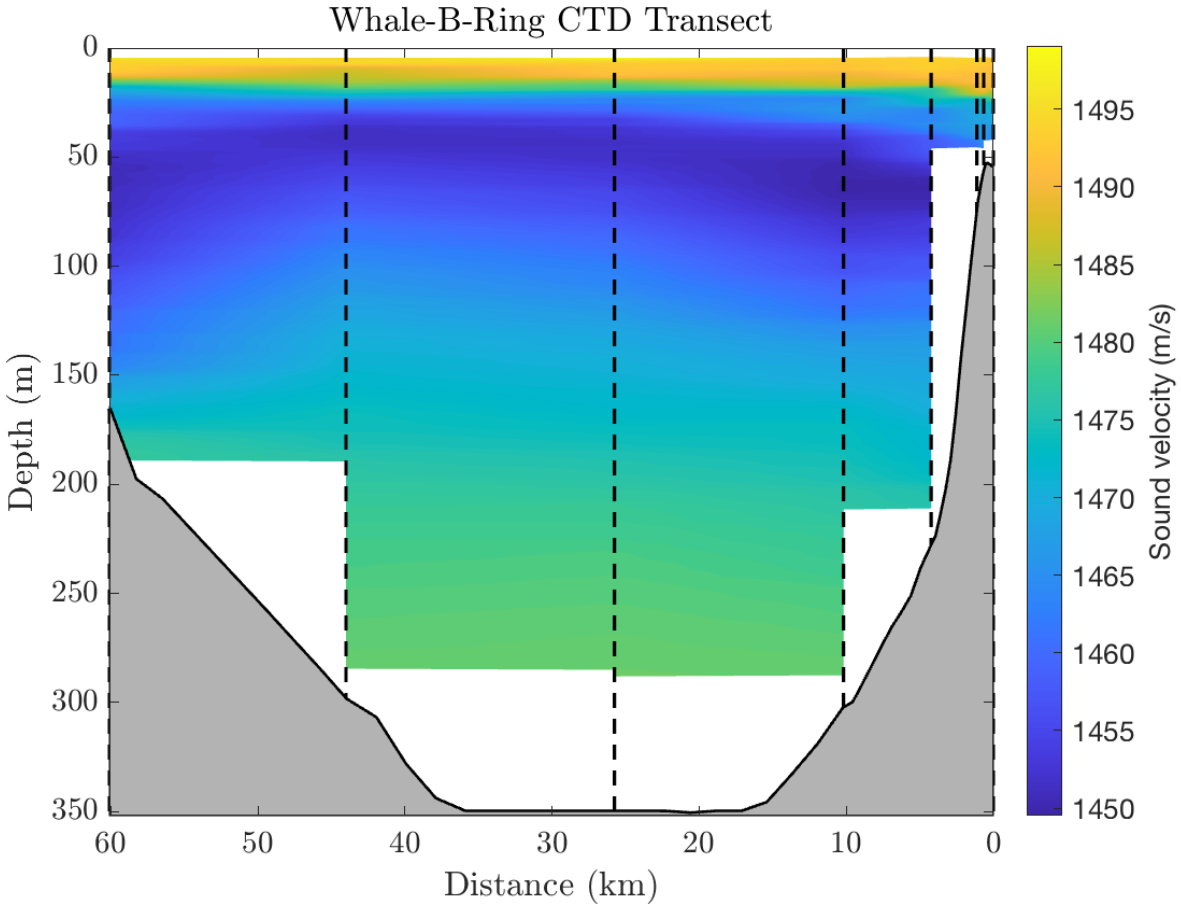

Figure 27. Cross-section of sound-speed on the transversal CTD transect in between the array pairs in Honguedo strait.
CTD profiles are positioned on Figure 26. Gaspé peninsula coast is on the right. Times and coordinates are provided in Table 5.

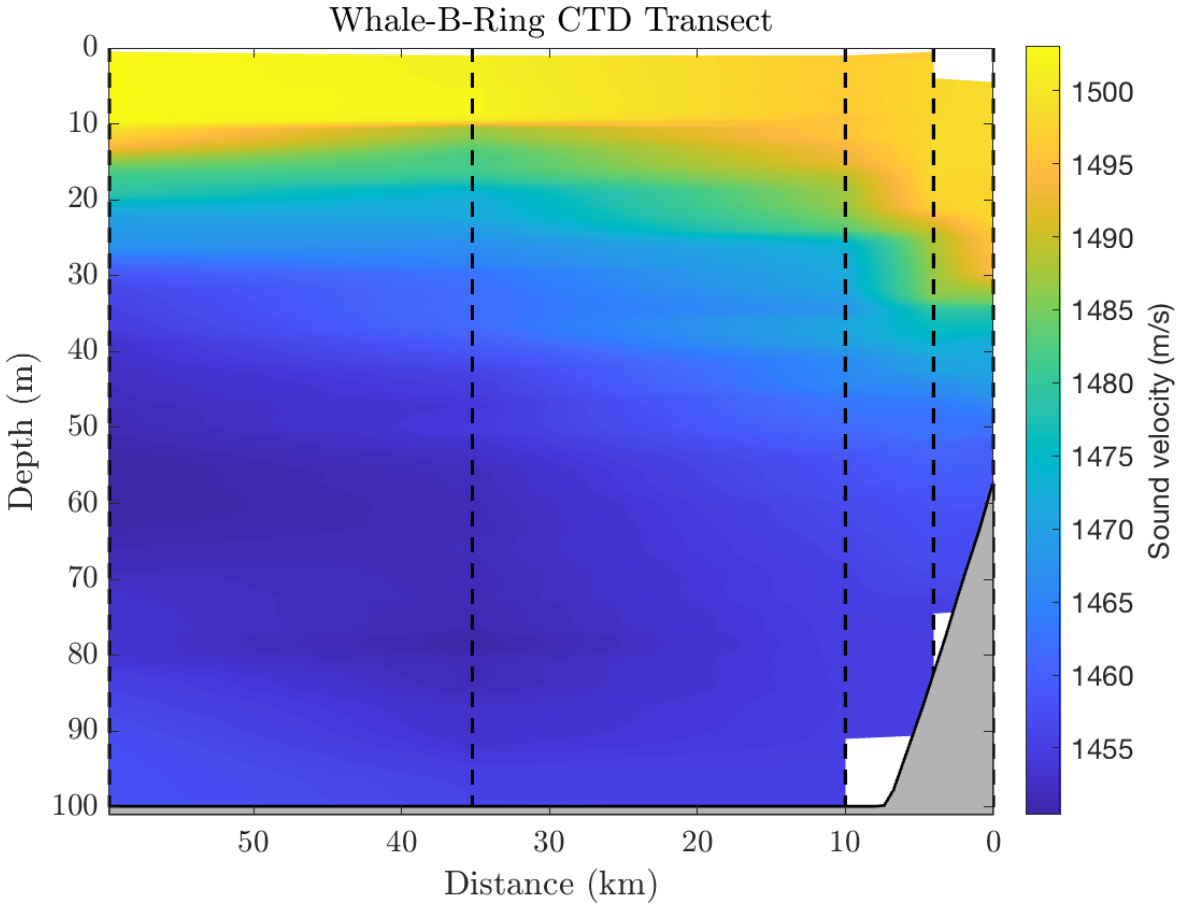

Figure 28. Cross-section of sound-speed on the transversal CTD transect in between the array pairs in Gaspé region.
CTD profiles are positioned on Figure 26. Gaspé peninsula coast is on the right. Times and coordinates are provided in Table 5.

Table 4. Positions and time of each set of sound emissions.

Station name	Pattern	Longitude		Latitude		Date and time
		Deg.	min	Deg.	min	(UTC)
Anse-à-Valleau	Ring	64	32.604	49	5.532	2021-07-15 18:05:02
		64	32.454	49	5.670	2021-07-15 18:08:44
		64	32.220	49	5.718	2021-07-15 18:11:00
		64	31.968	49	5.670	2021-07-15 18:14:00
		64	31.818	49	5.532	2021-07-15 18:16:20
		64	31.824	49	5.358	2021-07-15 18:18:58
		64	31.974	49	5.226	2021-07-15 18:21:37
		64	32.220	49	5.178	2021-07-15 18:25:15
		64	32.460	49	5.232	2021-07-15 18:27:56
		64	32.610	49	5.364	2021-07-15 18:30:12
Cloridorme	Ring	64	50.280	49	11.505	2021-07-15 14:19:17
		64	50.268	49	11.670	2021-07-15 14:22:36
		64	50.106	49	11.808	2021-07-15 14:25:50
		64	49.890	49	11.862	2021-07-15 14:29:00
		64	49.644	49	11.802	2021-07-15 14:32:00
		64	49.488	49	11.670	2021-07-15 14:34:22
		64	49.482	49	11.496	2021-07-15 14:37:00
		64	49.638	49	11.370	2021-07-15 14:39:42
		64	49.876	49	11.321	2021-07-15 14:42:00
		64	50.133	49	11.371	2021-07-15 14:46:00
	Ring center	64	50.268	49	11.586	2021-07-15 14:51:00
Honguedo	Parallel 1	65	21.168	49	28.440	2021-07-14 20:30:16
		65	6.360	49	23.262	2021-07-14 21:47:13
		64	55.458	49	19.548	2021-07-14 22:47:00
		64	48.006	49	17.016	2021-07-14 23:29:00
		64	43.026	49	15.300	2021-07-15 15:08:51
		64	37.206	49	13.272	2021-07-15 15:22:21
		64	31.379	49	11.258	2021-07-15 15:35:57
		64	26.278	49	9.497	2021-07-15 15:47:38
		64	19.020	49	6.967	2021-07-15 16:02:20
		64	8.127	49	3.149	2021-07-15 16:26:30
	Parallel 2	63	58.080	49	15.252	2021-07-14 11:44:00
		64	9.216	49	19.026	2021-07-14 12:46:00
		64	16.464	49	21.594	2021-07-14 13:27:00
		64	21.582	49	23.256	2021-07-14 14:02:00
		64	33.486	49	27.312	2021-07-14 15:05:00
		64	38.478	49	29.094	2021-07-14 15:33:00
		64	45.576	49	31.674	2021-07-14 16:15:00
		64	56.688	49	35.412	2021-07-14 17:14:00

Station name	Pattern	Longitude		Latitude		Date and time
		Deg.	min	Deg.	min	(UTC)
		65	11.496	49	40.218	2021-07-14 18:27:00
	Perpendicular	64	40.854	49	8.424	2021-07-13 23:50:00
		64	40.866	49	8.772	2021-07-15 00:25:00
		64	40.656	49	8.982	2021-07-15 00:38:42
		64	39.396	49	10.428	2021-07-15 01:11:00
		64	37.074	49	13.302	2021-07-15 01:58:00
		64	31.170	49	20.694	2021-07-15 03:26:59
		64	24.732	49	29.484	2021-07-14 05:01:47
		64	17.916	49	37.170	2021-07-14 06:21:16
Perce	Ring	64	11.904	48	32.136	2021-08-01 13:40:37
		64	11.670	48	32.088	2021-08-01 13:43:17
		64	11.526	48	31.956	2021-08-01 13:45:55
		64	11.514	48	31.788	2021-08-01 13:47:41
		64	11.670	48	31.650	2021-08-01 13:49:34
		64	11.916	48	31.602	2021-08-01 13:51:11
		64	12.144	48	31.662	2021-08-01 13:53:06
		64	12.294	48	31.788	2021-08-01 13:54:44
		64	12.288	48	31.950	2021-08-01 13:56:17
		64	12.144	48	32.094	2021-08-01 13:57:58
	Ring center	64	11.946	48	32.838	2021-08-01 14:00:45
Mal-Bay	Ring	64	11.178	48	36.504	2021-08-01 14:30:15
		64	10.944	48	36.456	2021-08-01 14:32:14
		64	10.800	48	36.318	2021-08-01 14:34:23
		64	10.794	48	36.150	2021-08-01 14:36:24
		64	10.938	48	36.012	2021-08-01 14:38:12
		64	11.778	48	36.156	2021-08-01 14:39:55
		64	11.418	48	36.324	2021-08-01 14:41:29
		64	11.568	48	36.156	2021-08-01 14:43:42
		64	11.556	48	36.324	2021-08-01 14:45:00
		64	11.418	48	36.456	2021-08-01 14:48:48
	Ring center	64	11.172	48	36.234	2021-08-01 14:49:05
Gaspe	Parallel 1	63	49.222	49	3.971	2021-07-31 13:58:40
		63	53.890	48	53.609	2021-07-31 15:14:13
		63	57.178	48	45.812	2021-07-31 16:15:47
		63	59.396	48	40.637	2021-07-31 17:02:58
		64	0.974	48	36.993	2021-07-31 17:36:58
		64	4.453	48	28.685	2021-07-31 18:43:00
		64	5.992	48	25.028	2021-07-31 19:15:20
		64	8.145	48	19.851	2021-07-31 20:00:26
		64	11.507	48	12.093	2021-07-31 21:00:53
		64	15.750	48	1.640	2021-07-31 22:18:43

Station name	Pattern	Longitude		Latitude		Date and time
		Deg.	min	Deg.	min	(UTC)
	Parallel 2	63	56.064	47	57.881	2021-08-01 02:52:58
		63	51.638	48	8.324	2021-07-31 04:30:09
		63	48.419	48	16.094	2021-07-31 05:46:34
		63	46.268	48	21.291	2021-07-31 06:38:48
		63	44.738	48	24.952	2021-07-31 07:20:10
		63	41.214	48	33.225	2021-07-30 19:23:20
		63	39.742	48	36.692	2021-07-31 08:56:26
		63	37.461	48	41.925	2021-07-31 09:44:19
		63	34.192	48	49.778	2021-07-31 10:45:10
		63	29.629	49	0.179	2021-07-31 12:08:11
	Perpendicular	64	9.038	48	33.981	2021-07-30 14:08:00
		64	7.438	48	33.675	2021-07-30 14:21:48
		64	7.902	48	33.682	2021-07-30 14:31:58
		64	6.714	48	33.570	2021-07-30 14:40:20
		63	42.983	48	29.060	2021-07-30 18:31:00
		63	23.851	48	26.719	2021-07-30 21:21:27

Table 5. Positions of the CTD profiles along the perpendicular transects

Station	Longitude		Latitude		Date and time	Depth
	Deg.	min	Deg.	min	(UTC)	(m)
RED1	64	40.777	49	8.410	2021-07-14 00:03	54
RED2	64	40.846	49	8.751	2021-07-14 00:13	70
RED3	64	40.656	49	8.972	2021-07-14 00:32	52
RED4	64	39.489	49	10.429	2021-07-14 00:57	225
RED5	64	37.143	49	13.288	2021-07-14 01:38	304
RED6	64	31.170	49	20.732	2021-07-14 03:04	386
RED7	64	24.139	49	29.453	2021-07-14 04:41	327
RED8	64	17.773	49	37.084	2021-07-14 06:07	202
Perp1	64	10.560	48	34.300	2021-07-30 13:50	80
Perp2	64	7.420	48	33.684	2021-07-30 14:26	99
Perp3	64	2.734	48	32.786	2021-07-30 15:06	117
Perp4	63	42.991	48	29.051	2021-07-30 18:27	146
Perp5	63	23.800	48	25.413	2021-07-30 21:38	116